THEORETICAL ANALYSIS OF A SOLAR AIR COLLECTOR WITH A RECTANGULAR AIR-DUCT PROFILE

BY

HEZBON OPITI ONDIEKI

SC/PGP/014/08

A THESIS SUBMITTED TO THE SCHOOL OF SCIENCE IN PARTIAL FULFILMENT OF THE REQUIREMENT FOR THE DEGREE OF MASTER OF SCIENCE IN PHYSICS OF UNIVERSITY OF ELDORET

APRIL, 2012

TITLE

DECLARATION

DECLARATION OF THE CANDIDATE

This thesis is my original work and has not been presented anywhere for research leading to a degree in any University. No part of this thesis may be reproduced without the prior written permission of the author and/or The University of Eldoret

Ondieki O. H.: Sign..... Date.....

SC/PGP/014/08

DECLARATION BY THE SUPERVISORS

This thesis has been submitted to the School of Science with our approval as university supervisors.

Dr. J. K. Tonui: Sign..... Date: .....

Head of Department,
Department of physics,
The University of Eldoret

Prof. S. K. Rotich: Sign..... Date: .....

Department of physics,
Moi University

DEDICATION

This thesis work is dedicated to my late grandmother whose words of encouragement and push for tenacity ring in my ears. From you, I learned that the best kind of knowledge to have is that which is learnt for its own sake and even the toughest task can be accomplished if it is done one step at a time. To my beloved son, Alvan Ondieki, "*Your smile, hope and trust in me always re-energizes the fighting spirit of the many challenges in life."* I hope this will teach you to work hard for things that you aspire to achieve. Now, I pass on a baton of love and passion for reading and respect for education to you. To my dear wife Zipporah Moraa for your prayers, care, moral and financial support, patience, understanding, encouragement and unconditional love. I am truly thankful for having you in my life. Hoping that with this research I have proven to you that there is no mountain higher to climb as long as God is on our side. "*No matter the challenges, our destiny is valid*."

ABSTRACT

Any solar energy conversion system requires proper designing and sizing in order for it to be cost effective with respect to energy production under the prevailing climatic conditions and initial cost. Modelling and simulation have been considered as fast and cheap analytical tools for sizing of optimal solar energy systems for a given application prior to their construction. This work provides a theoretical analysis of a solar air heater (SAH) with a rectangular air duct profile and operated under natural airflow mode. The model was validated against experimental results measured outdoors on a prototype model. The validation results showed a good agreement between experimental and modelling results hence the model could be used for analytical analysis of this type of SAH system. The model was used to study the effects of various operating conditions and design parameters on the performance of SAH. The results show that increase of mass flow rate, solar insolation and collector area increases the efficiency of the SAH system. The optimal values of efficiency are obtained when the mass flow rate is greater than 0.01 kgs^{-1} and around mid-day when the insolation rate is greater than 1000 W/m^2. It was also observed that the efficiency of the collector increases with increase in both the collector length and width and attains its optimum values of efficiency between 1.0 to 2.0 m for both length and width. In addition, better performances of the collector are obtained at low ambient temperatures and small channel depths.

TABLE OF CONTENTS

CONTENT **PAGE**

LIST OF TABLES **PAGE**

LIST OF FIGURES **PAGE**

SYMBOLS AND ACRONYMS

SYMBOLS

A Surface area of the collector (m^2)

C_p Specific heat capacity of air at constant pressure ($Jkg^{-1}K^{-1}$)

T_a Ambient temperature (^0C)

T_p Plate temperature (^0C)

T_{out} Output temperature (^0C)

T_{in} In-let temperature (^0C)

T_f Average air temperature (^0C)

T_g Glass temperature (^0C)

T_s Sky temperature (^0C)

U_L Overall heat loss coefficient (W/m^2K)

U_t Top heat loss coefficient (W/m^2K)

U_b Back heat loss coefficient (W/m^2K)

V Wind velocity (m/s)

h_c Convection heat coefficient (W/m^2K)

h_{rp-g} Radiation heat loss coefficient from plate to glass (W/m^2K)

h_{rg-s} Radiation heat loss coefficient from plate to sky (W/m^2K)

h_w Wind convection heat loss coefficient (W/m^2K)

F_R Heat removal factor for solar air heater

I Plane of array solar radiation (Wm^{-2})

Q_u Rate of useful heat gain collected by the air (W)

Q_{cond} Rate of conduction heat loss from the absorber (W)

Q_{conv} Rate of convection loss from the absorber (W)

Q_R Radiation heat loss from the absorber (W)

Q_ρ Rate of reflection heat loss from the absorber (W)

Q_L Total heat loss from the collector (W)

ρ The reflection coefficient of the absorber

α_p Absorptivity of the absorber plate

$\dot{m}$ Mass flow rate (kgs^{-1})

τ The transmittance of the glass cover

S Solar radiation absorbed by the collector plate (W/m^2)

η Efficiency (%)

v Kinematic viscosity (m^2/s)

σ Stefan–Boltzmann constant (W/m^2K^4)

ε_g Emmisivity of glass

ε_p Emmisivity of the absorber plate

d Insulation thickness (m)

k_i Thermal conductivity of insulation (W/mK)

k Thermal conductivity of air (W/mK)

Nu Nusselt number

L	Channel depth (m)
D_h	The hydraulic diameter (m)
W	Collector width (m)
β	Thermal expansion coefficient (K^{-1})
g	Acceleration due to gravity (ms^{-2})
θ	Collector tilt angle (degrees)

ACRONYMS

SAH	Solar Air Heater
RD&D	Research Development and demonstration
PV	Photovoltaics
SHP	Solar Heat Power
PCM	Phase Change Material

ACKNOWLEDGEMENT

First and above all, I praise God the almighty, for providing me this opportunity and granting me the strength and capability to proceed successfully. It is with immense gratitude that I acknowledge the support and help of my supervisors Dr. J. K. Tonui and Prof. S. K. Rotich for their encouragement and helpful discussions which guided me in writing this thesis. I greatly learned more from your experience in the field of science to see the insight of the area of study. I want to express my deepest gratitude to Mr Martim for his experimental work than I used to validate my work. I also share the credit of my work with the entire staff of Physics Department for their support and understanding that created an enabling environment for research. To my colleagues pursuing Msc. in the department of physics at The University of Eldoret, *"Kudos",* your inspiration was commendable in writing of this thesis.

A special thanks to my family. Words cannot express how grateful I am to my late Grandmother (Norah Nyomenda) for all of the sacrifices that she made on my behalf. I warmly thank and appreciate my mother (Esther Kerubo), brothers (Denis and Edwin), Sisters (Getrude and Maurine), uncles (Elijah and Zablon), aunties (Jane and Agripha) and the entire family whose help, steadfast love, support and encouragement was of great help in my studies. Your prayer for me was what sustained me this far. Above all, *I owe my deepest gratitude* to my Lovely wife for her personal support and great patience at all times. My dear "*you were my support in the moments when there was no one to answer my queries, you have been patient with me when I'm frustrated, you celebrate with me even when the littlest things go right, and being there whenever I needed you to just listen."* Thank you for your unequivocal support throughout, as always, for which my mere expression of thanks likewise does not suffice. I just say thanks for everything and may God give you all the best in return. I hope I will make all of you proud. May God bless you all.

CHAPTER ONE

INTRODUCTION

1.1 Background of study

Energy is the primary and universal measure of all kinds of natural or human activities. Everything that happens in the world is the expression of flow of energy in one of its many forms. We use it to heat and light our homes, to power appliances in our businesses and to transport people and goods from one location to another. Plants on the other hand utilize solar energy to manufacture their own food during photosynthesis. Without a clean, secure and sufficient supply of energy we would not be able to function as an economy or as a modern society. In any energy delivery, the energy sector in the world today is facing two main challenges. The first challenge is to meet the ongoing exponential growth in demand for energy services due to the ever growing world population, especially in the developing countries, where 80% of the two billions people in the world without electricity live. The increasing demand for energy in many developing countries is also accelerated by the improving social-economic and industrial developments as well as the people's change of life style. All these sectors require electrical energy for their operation and are likely to cause strains in the existing electrical energy supply because the production level may not be commensurate with the level of demand.

The second challenge faced by the energy sector is to deal with the local, regional and global environmental effects resulting from the supply and use of energy. Climate

change represents a significant risk to the global ecosystems, the world economy and human populations. In the year 2007, the Intergovernmental Panel on Climate Change (IPCC, 2007) published a report which stated that "warming of the climate system is unequivocal" and that "most of the global average warming over the past 50 years is very likely due to anthropogenic green house gases (GHG) increase". It also warned that "unmitigated climate change would, in the long term, be likely to exceed the capacity that natural and human systems can adapt". In order to lower the amount of GHGs emission into the atmosphere, it is imperative to look for ways to either improve consumption efficiencies of the conventional energy sources or seek alternative benign sources of energy. The conventional fossil fuel combustion releases carbon dioxide and other greenhouse gases into the atmosphere which leads to global warming, acidic rain and air pollution. In addition, the production and transportation processes may result in damage to the ecosystems through dredging or spillages (Choudhury, 2002). For instance, the oil spill in the wells of the Gulf of Mexico in the year 2010 flowed for three months causing extensive damage to marine and wildlife habitats as well as the negative impacts on the Gulf's fishing and tourism industries. In addition, the explosion killed 11 workers and injured 17 others (Deepwater horizon oil spill, retrieved on 20th December 2010 - *www*.en**.***wikipedia***.**org/*wiki/Deepwater_Horizon_oil_spill* **).**

As governments in many countries grapple with rapid growth in energy demand and equally pressing sustainability constraints, renewable energy technologies are increasingly viewed as strong contributors to the solutions. The "alternative scenario" presented in the International Energy Agency's world energy outlook 2004 (IEA, 2004)

demonstrates clearly that implementation of more vigorous national environmental and energy-security policies, together with faster deployment of appropriate technologies, would lead the world towards a better energy future. Moreover, renewable energy technologies are seen as the basic components in measures to eradicate poverty. New technology solutions are viewed as a bridge to many sustainability gaps for the immediate future. For the longer term, whole new generations of sustainable energy technology must emerge if the objective of greater energy security and protection of both local environment and worldwide climate is to be attained. Every technology avenue must therefore be explored to provide options for the gradual transition towards energy systems for the longer term that can simultaneously meet the maximum number of economic, social and environmental goals. Many of the necessary technologies for the nearer term are moving towards cost competitiveness.

According to the United States congress office of technology assessment (1992), the energy sector has undergone several stages of evolution and development. However, the fossil fuel has remained to be the major source of energy to many countries in the world up to now. The over-dependence on the natural resource of oil and gas from the finite world reserves has resulted to its gradual depletion and the situation is becoming more visible with time. This has made many governments in the world today to embrace paradigm shift in energy supply from conventional to renewable, especially in industrialised countries. Furthermore, this shift is gaining momentum due to the rising world oil prices, especially in oil importing countries and the impacts of climate change. In the new dispensation, the renewable energy sources are not only expected to

supplement the conventional sources in the short term but to replace them altogether in future.

Renewable energy sources are envisaged to reduce the gap between the energy demand and supply because of their enormous potential and diversity. They can enhance diversity in energy supply markets, secure long-term sustainable energy supplies, and reduce local and global emission of atmospheric gases. They can also provide commercially attractive options to meet specific needs for energy services in rural settlements in both developed and developing countries and create new employment opportunities. However, there is still a need for more RD&D to be done to improve the conversion efficiencies of the various renewable technologies whose conversion efficiency are still low in order to reduce cost and make them more competitive with their counterpart for wider acceptance and applications.

The renewable sources of energy include nuclear energy, mini- and micro-hydropower, tidal energy, biomass, wind power and solar energy. Nuclear energy is one of the sources that release a large amount of energy as a result of the nuclear fission of atoms such as uranium and plutonium. However, high costs of production, proliferation of nuclear weapons and ongoing concerns about the nuclear waste disposal and management of accidental leakages from nuclear power plants, has made this source to be explored by few countries in the world, mainly in developed countries and in particular France who generate over 75% of her electricity from nuclear energy, (World Nuclear Association,2011). Usually, the leakages from the nuclear power plants cause huge

economical loss to the country and great environmental negative effects to the areas surrounding the plant. For instance, the most recent disaster at Fukushima Daiichi Nuclear Power Plant in Japan resulted to great repercussions to the economy and the people's health (Josie Garthwaite, 2011).

Mini- and micro-hydropower use water as a raw material for energy generation. Mini-hydroelectric power plant is a small power station that is able to produce relatively small amounts of electricity (usually with capacity of less than 10 MW) as compared to large hydro-electric power plants (Maser, 2009). The development of mini-hydroelectric power is being promoted as an alternative source of electricity for local industries and communities where there are suitable sites for its construction because in most parts of the world, it is not possible to find rivers with enough water capacity to sustain setting up large power plants. Tidal energy is also another type of source of energy that utilizes water as main raw material. It is harnessed mainly along the coastal regions where there are ocean tides. Tidal energy is obtained from the changing of sea levels i.e. a direct result of tide shifting from low to high. The research on tidal energy in the recent past is intensifying because this source of energy is seen to be predictable since the tides can be predicted centuries into the future. Tidal currents normally follow a daily cycle and will not be affected by global climate change. Based on tidal modelling studies, environmental and physical impacts of tidal current power generation are small. However, tidal energy could only be harnessed in places with significant water level changes (Maser, 2009).

Biomass is usually used directly in form of wood fuel, animal waste and agricultural wastes in most households in rural areas and by low income earners in urban centres as the main source of energy for cooking, heating and in some cases lighting. Though, the direct use of biomass seems to be relatively cheap and easily accessible, it is not a clean source of energy as it releases smoke that can be a problem in poorly ventilated houses, time consuming in gathering and also leads to the depletion of forest cover. New technologies have been developed recently for conversion of biomass into portable and commercial form of energy with high thermal conversion efficiency such as biodiesel, methanol, ethanol, di-methyl esters, pyrolytic oil and Fischer-Tropsch gasoline (IPCC, 2001). In addition, crop and wood residues, animal and industrial organic wastes are currently used to generate biogas for cooking in commercial places. In the year 2001 (IEA, 2001; Smeets and Faaij, 2007) global biomass energy use for cooking and heating was only 9.3% of the global primary energy use, and biomass energy use for electricity and fuel generation was only 1.4% of global primary energy use.

Wind power involves the use of the wind kinetic energy to turn the wind turbines that generate electricity or drive wind mills and pumps as well as driving the sails that propel ships. Wind energy is one of the safe sources of energy and can be harnessed in most locations where there is high wind potential. However, the construction of wind farms may not be universally welcomed because of its running cost due to maintenance of the moving parts as well as visual impact of the huge turbines and noise they produce. The high initial cost of the equipments may also contribute to their unpopularity.

Solar energy is among the sources that have been under intense exploration in the recent past and most promising form of renewable energy that is projected to meet the world energy demand. There are many useful applications of the solar energy in day-to-day life, either directly (by open sun heating and drying or by use of solar technologies like solar thermal and Photovoltaic systems) or indirectly (as wind, biomass, hydropower and or geothermal power). Solar energy is available everywhere though with varying quantities depending on the geographical location, season and time of the year. It will practically never run out so long as the sun shines and is available under all weather conditions, even during overcast conditions as in winter seasons. In addition, solar energy is completely free as far as the resource itself is concerned. According to Muguti (2001) and Gashie (2006), using the sun's energy is no longer wishful thinking from idealists of environmental sustainability, but a solution to the world's challenge in the energy sector. They emphasize the need for funding in the exploration and development of better and efficient solar collectors to harness sufficient solar energy.

Solar energy can be utilized directly as thermal energy or as electrical energy. Solar thermal conversion, involves the use of solar thermal collectors to convert the incident solar radiation into heat energy. The solar thermal collectors are usually flat-plate collector systems or concentrator systems. They absorb as much as possible of the incoming solar radiation and delivers a high fraction of the captured energy through a working fluid, usually air or water, directly into the point of application or into a heat storage system for later use.

Solar air heater (SAH) is one of the major solar thermal systems that are under intense exploration and its use has gained momentum in most developed countries due to its wide range of applications. A SAH is a solar thermal collector that uses ambient air as a heat removal medium. The heated air is then used for such applications as space heating and ventilation in buildings or for drying purposes in both industrial and agricultural sectors. In Africa, these systems are mainly used for drying agricultural products. The SAH systems are simple in design and can operate under natural convection or forced convection. In addition, they do not need protection from corrosion, freezing or boiling conditions. However, these systems have low thermal conversion efficiencies due to poor thermal-physical properties of air such as thermal conductivity, specific heat capacity, density and dynamic viscosity. Therefore, there is need for more research on ways of increasing the heat transfer coefficients to improve the thermal efficiency of the SAH systems in order to make them economically viable.

The use of the SAHs in most developing countries, especially in Africa, is also very low as compared to developed countries. This is attributed to the prevailing high solar radiation, which makes the traditional open sun drying a cheaper and direct option. In addition, the SAH systems are not available in the market and there is lack of awareness on the potential of SAH systems for drying among the prospective users. This also calls for more RD&D projects on SAH systems in Africa to enhance awareness among farmers on the benefits of using SAHs for drying agricultural products over traditional open air drying methods and provide them with new or innovative way of installing them.

1.2 Statement of the Problem

Solar air heater (SAH) is a major solar thermal system that is used to tap the heat energy from the solar radiation for a wide range of applications. In Africa, SAH systems are suitable for use in drying of crops (mainly cereals, fruits, vegetables and tobacco, medicinal plants and fish) in agricultural sector (Gatea, 2010) since the systems can provide a cheaper and cleaner method of drying the crops throughout all seasons (Abdullah and Gatea 2011). However, the use of solar air heaters in Africa is not a common phenomenon, and farmers still use the traditional open-air drying methods which exposes famers to risks of incurring huge post harvest loses mainly as a result of contamination and spoilage of crops by pests, livestock and rain. The low number of SAH systems in operation in Africa is attributed mainly to lack of awareness among prospective users on their potentials, and benefits as lack of technical knowhow on their installation among the prospective users. Currently, there are a few RD&D projects on SAH systems especially in Africa, which are necessary for wider awareness and dissemination of any new or innovative technology worldwide.

1.3 Objectives of the study

1.3.1 General Objectives

The general objective of this study was to develop a mathematical model and use it to analyze the performance of a prototype solar air heater (SAH) system designed, constructed and tested outdoor at the Department of Physics, University of Eldoret.

1.3.2 Specific Objectives

The specific objectives of the study were:

1. To develop a mathematical model based on the energy balance equations of the SAH system.
2. To investigate the effect of changes in the design parameters (length, width and channel depth) and operating conditions (flow rate, ambient temperature and insolation) on the SAH system thermal performance.

1.4 Justification of the Study

In many parts of the world, there is a growing awareness among the farmers that renewable energy technologies play important role in improving the yield and quality of crop production. However, the application of renewable energy in improving crop production, especially in post harvest stage, has not been fully exploited despite being endowed with vast resources of these energy sources. Solar thermal technology is a technology that is rapidly gaining acceptance as an energy saving measure in agricultural application because it provides practical solutions to the problems associated with provision of energy that is of low cost and environmentally benign. The use of SAH

systems for crop drying is the most suitable application in developing countries because most of their economies are agriculturally driven. However, there is little use of these systems in such application because of lack of awareness on their potentials. Therefore, there is a need for more research and demonstrations projects to create awareness and provide information on the potential of SAH systems in provision of hot air required to dry crops. The SAH systems ensure quality post harvest preservation and storage of food crops which in turn ensures food security and good health of the people.

CHAPTER TWO

LITERATURE REVIEW

2.1 Introduction

This chapter discusses the theoretical concepts concerning solar air heaters. The theoretical equations that are useful for the development of the numerical model for the system are also given.

2.2 Solar Energy

Solar energy is radiant energy that is emitted by the sun. Everyday the sun radiates out an enormous amount of energy. There is a general belief among researchers that the sun produces enough solar energy in one day to power the entire energy requirements of the whole world for a year. The plants convert sunlight into chemical energy by means of photosynthesis and this energy sustains the life of the plants themselves and the animals that feed on them. On the other hand, since time immemorial, man has utilized the solar energy directly as a source of heat for warming and drying applications in their everyday life. Solar energy has also been used by mankind indirectly in form of fossil fuels, biomass and wind power.

2.3 Solar Radiation

Solar radiation is an electromagnetic radiation emitted by the sun, which span from ultra-violet radiation to infrared radiation of the electromagnetic spectrum. The amount of solar radiation received at the earth's surface (terrestrial radiation) is lower than that received outside the atmosphere (extraterrestrial radiation) due to attenuation as it passes through the earth's atmosphere (see Fig. 2.1).

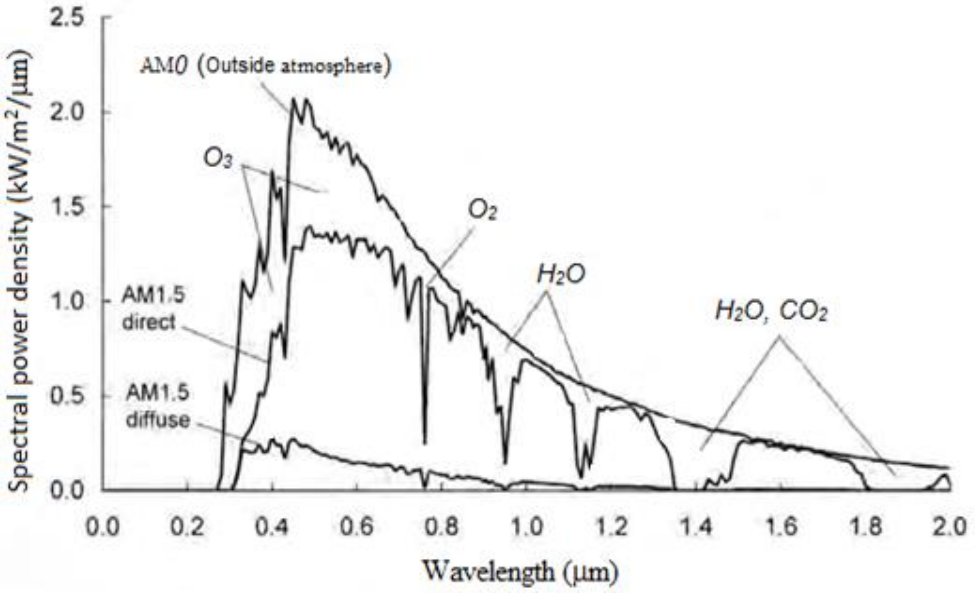

Fig. 2.1: The spectral power density of sunlight at AM0 and AM1 (Gueymard, 2004)

The attenuation is caused by absorption and scattering of solar radiation by atmospheric gases and other aerosols in the atmosphere (see Fig. 2.2). Absorption occurs primarily because of the presence of ozone layer, clouds and water vapour in the atmosphere and to a lesser extent due to other gases (like CO_2, NO_2, CO, O_2 and CH_4) and particulate matter in the atmosphere. The ozone absorbs mainly the ultraviolet radiation with wavelengths below 0.3 μm. Depletion of ozone from the atmosphere allows more ultraviolet radiation to reach the earth's surface, which consequently has harmful effects upon biological systems. The gases, CO_2, NO_2, CO, O_2 and CH_4 molecules contribute to the absorption of infrared solar radiation. By changing their content in the atmosphere, the absorption of the infrared solar radiation is influenced, which has consequences on the earth's climate (The Concise Columbia Electronic Encyclopaedia, 1994).

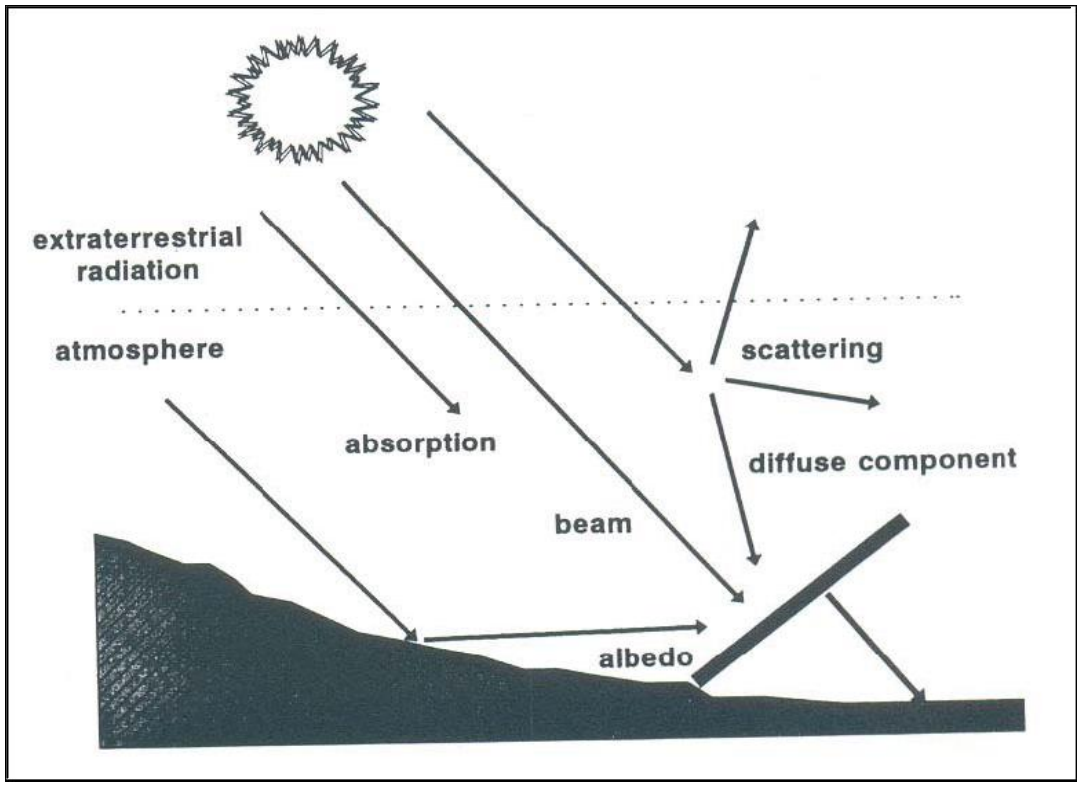

Fig. 2.2: Schematic representation of the beam, diffuse and albedo radiations received on an inclined plane at the earth's surface.

On the other hand, scattering occurs due to the interaction between the solar radiation with all gaseous molecules, water vapour and aerosol in the atmosphere. The air molecules, water droplets and aerosols scatter radiations in the visible region with wavelengths comparable to their sizes through the Rayleigh scattering process. The scattered radiation is redistributed in all directions, some going back into space and some reaching the earth's surface. The solar radiation that is received directly on a collector on the earth's surface is called direct or beam solar radiation. On the other hand, the radiation that is intercepted after scattering or at angle is called diffuse solar radiation. The sum of

the direct and diffuse solar radiation received on a horizontal plane on the earth's surface is called global solar radiation. Practical solar collectors are normally installed on tilted surfaces bringing in another component of incident solar radiation called albedo radiation. Albedo radiation is the proportion of the solar radiation that is reflected by the earth's surface. Thus, for tilted surfaces, the global solar radiation consists of three components: beam, diffuse and albedo radiation (Duffie and Beckmann, 1991; Norton, 1992).

The common instruments used to measure the solar radiation are pyranometers and pyrheliometer. The pyranometer is used to measure the global hemispherical solar radiation received on a surface. The pyranometer can also be used to measure the diffuse solar radiation by blocking the direct component using a shading element, usually called a shading ring. The shading ring is positioned along the polar axis at an appropriate distance from the sensor. The knowledge of horizontal global and diffuse solar radiation obtained from the pyranometer can be used to calculate the direct solar radiation (Duffie and Beckmann 1991; Garg and Garg, 1993).

The direct solar radiation can also be measured directly using a pyrheliometer. The pyrheliometer is a telescopic type of instrument with a narrow aperture which allows only radiations at normal incidence to reach the sensor. The pyrheliometer is mounted on a Solar Tracker or an Automatic Solar Tracker which makes the instrument face the sun and follows its motion for continuous readings (Duffie and Beckmann 1991; Garg and Garg, 1993).

2.4 Factors that affect the radiation that falls on the Earth's surface

Every location on the earth receives sunlight daily throughout the year though with varying intensity and duration. The amount of solar radiation that reaches any one "spot" on the Earth's surface varies according to the following factors:

- Geographic location
- Time of the day
- Season of the year
- Local landscape
- Local weather

The sun's rays strike a surface at different angles ranging from 0º (just above the horizon) to 90º (at zenith) because the Earth is spherical. When the sun's rays are vertical, the Earth's surface gets the maximum energy possible. The more inclined the sun's rays are, the longer they travel through the atmosphere, becoming more scattered and diffuse. The Earth revolves around the sun in an elliptical orbit. This makes it to be closer to or far from the sun during part of the year resulting to the four seasons. In a year, some parts of the earth (Polar Regions) never receive a high solar radiation, and because of the tilted axis of rotation, these areas receive no sun at all during part of the year. The tilting normally results to longer days in the northern hemisphere from the spring (vernal) equinox to the fall (autumnal) equinox and longer days in the southern hemisphere during the other six months. The days and nights are both exactly 12 hours long on the equinoxes, which occur each year on or around March 23 and September 22 (Duffie and Beckman, 1991).

In the regions lying within the tropics, like Kenya, the sun is almost overhead throughout the year whereas regions outside the tropics or in high latitudes, receive more solar energy during the summer season than in winter season as a result of having longer days and the sun being nearly overhead during the summer days. The rotation of the Earth also determines the hourly variations in sunlight reaching the earth's surface because it determines the position of the sun during the day resulting to morning, noon and evening. The sun's rays usually travel longer distances through the atmosphere when the sun is at the horizon (morning and evening) covering a large air mass than at noon when the sun is at zenith. This results to the earth receiving high amount of solar radiation at noon as compared to morning and evening. The other factor that affects the solar radiation intercepted at the earth's surface is the kind of weather conditions during the day. The earth usually receives the highest amount of solar radiation during a clear day (cloudless) than a cloudy day because the cloud cover increases the attenuation process of solar radiation which makes the earth to receive low and almost constant solar radiation during a cloudy day (Norton, 1992).

2.5 Technologies for Harnessing Solar Energy

The solar energy is utilized either as heat energy or electricity. Since the solar radiation reaching the surface of the earth has undergone the process of attenuation, it needs to be collected and concentrated because of its dilute nature. This process involves the use of devices that collect and concentrate the incident solar energy to a level that is useful for the intended application.

2.5.1 Solar Electricity

Solar energy can be used to generate electricity in two ways: photovoltaics (PV) or solar heat power (SHP). Photovoltaic is the process of generating electricity directly from sunlight using photovoltaic or solar cells. These cells are made up of large area semiconductor diodes, such as crystalline silicon and gallium arsenide. The solar cells convert solar radiation directly into electricity by the process of photovoltaic effect. Photovoltaic cells produce a direct current (dc) which can be converted to alternating current (ac) if necessary using inverters. A single photovoltaic cell by itself cannot generate enough electricity for practical use. Therefore, many cells are normally connected in series and parallel electrical networks to produce a desired power output. When the solar cells are combined in this way, they form a solar or PV panel or modules. The panels can also be connected in series or parallel to form arrays that can generate even larger power. The current produced is directly dependent on the intensity of light reaching the module.

The solar thermal power, on the other hand, uses solar concentrators to focus the sunlight onto the point where a liquid is made to flow to generate steam which turns the turbines to generate electricity. Concentrating systems engage mirrors and lenses to focus the sun`s radiation to the collector, usually referred to as central receiver, where water or salt solutions are used to generate steam which is used to drive steam turbines that generates electricity. This technique is usually referred to as solar heat power (SHP).

2.5.2 Solar Thermal

Solar energy can be converted directly into thermal or heat energy using the solar thermal collectors. Solar thermal collectors are devises that absorb and transfer heat energy from the sun to a usable and or storable form in many applications. The major component of any solar thermal collector is the absorber plate. This is the part of the collector that intercepts and absorbs the incoming solar energy. The heat generated is then transferred convectively into a heat removal fluid, usually air or water. The heated fluid provides heat energy that can be used directly for water heating, space heating, power generation, ventilation, space cooling and refrigeration, distillation, drying, and cooking. The heat generated can also be stored in sensible heat storage systems (water or rocks) or latent heat storage systems using Phase Change Materials (PCM) for later use either at night or during cloudy days.

Solar thermal applications have been categorized into three broad categories depending on the range of temperature given out: low-temperature applications (below 80^{o}C), such as solar drying, space heating, ventilation and domestic hot water supplies, medium-temperature applications (between $80\ ^{o}$C - 150^{o}C), such as refrigeration, and cooking, and high-temperature (above 150^{o}C) applications for industrial processes (Duffie and Beckman, 1991; Sarkar and Obaidullah, 2006)

There are basically two types of solar thermal collectors depending on mode of operation: concentrating and non-concentrating. Concentrating solar thermal collectors employ lenses or concave reflecting surface to intercept and focus the sun's beam radiation to

small area (receiver), thereby increasing the radiation flux. The system of reflecting surface is installed with the reflectors set up either in continuous or segmented pattern. The receivers on the other hand maybe convex, flat, cylindrical or concave with or without a glass cover. Most of the concentrating collectors are installed with a solar tracking device which enables them to track the sun either from east to west or from north to south.

The non-concentrating collectors normally have the same area for intercepting and absorbing solar radiation. They are usually fixed and require no sun tracking. During installation, these collectors are oriented directly towards the equator, facing South for Northern hemisphere and North for the Southern hemisphere. The optimum tilt angle of the collector is equal to the latitude of the location with angle variation of $10^{o} – 15^{o}$ more or less depending on the application (Kalogirou, 2004). The inclination of the solar collector determines the incident solar irradiation on the aperture area and the heat loss through the front air layer between the absorber plate and cover glazing. Horizontal air layer with absorber at the bottom will show considerably higher Nusselt numbers (higher natural convection heat transfer coefficients) than air layer of vertical position (Matuska *et al.,* 2009). The non-concentrating solar thermal collector falls under two categories: Flat plate collectors and evacuated tube collectors. The most common non-concentrating solar thermal collectors in use are generally flat plate collectors.

A flat plate solar collector consists of a glazing material, an absorber plate and a back insulation material. The absorber plate is the heat exchanger of any solar thermal

collector. The absorbing material is usually desired to have a high absorptivity of the incident radiation, low thermal emissivity and good thermal conductivity. This is achieved by painting or coating the metallic or plastic absorber surfaces with ordinary black paint or using the selective surface coating. The absorber plate should also be stable thermally under all temperatures encountered during operation and stagnation. The absorber plates that are in use have different designs. They can be flat, corrugated or grooved plates, onto which the tubes, fins or passages are attached.

The glazing material is normally used to reduce convection and radiation losses from the collector system. The effective cover material should have a high transmittance of solar radiation in the visible range of the spectrum (short wavelength radiations) and a low transmittance to infrared radiation (long wavelength thermal radiation) in order to effectively trap in re-radiated heat from the absorber. The cover material should also have low absorptivity, be stable at all operating temperatures, durable under adverse weather conditions and of low cost. Glass has been widely used as covers of solar collectors because of its high transmitivity (as high as 90%) of the incoming shortwave solar radiation while transmitting virtually none of the long wave radiation re-emitted by the absorber plate. Glass with low iron content has a relatively high transmittance for solar radiation (approximately 0.85–0.90 at normal incidence), and very low transmittance to long wave thermal radiation (5.0–50 μm) emitted by the absorber plate (Kalogirou, 2004).

The collector systems also need to be well insulated against thermal heat losses from the absorber plate by conduction. This is usually achieved by putting the insulating foam

(such as polyurethane foam and Rockwool rubber seal) between the casing and rear part of the absorber plate and also side surfaces of the collector.

The solar thermal collectors that use fluid as heat transfer medium are classified as water-type and air-type solar collectors. Solar water heaters are used for heating water for use in residential or commercial premises. The dissemination of solar water heaters in Africa is still very low as compared to that in the developed countries. The main reasons for the low dissemination of these systems in Africa are the high initial cost for installation which is beyond the capability of most individuals and inadequate awareness on the use of solar water heaters. Solar air heaters are basically used for drying applications. In Africa, solar dryers are mainly used for drying fruits, vegetables and fish (Karekezi and Ranja., 1997; Karekezi, 2002; Karekezi *et al*. 2006; Kurtbas and Turgut, 2006). However, the use of solar dryers is also low in Africa. This is as a result of the favourable local weather conditions which encourage the use of open air drying method because Africa continent lies within the tropics where the sun is almost overhead throughout the year.

The solar thermal collectors can be operated as passive or active systems. The passive system is one which uses natural flow for the circulation of the heat transfer fluid while the active or forced flow system uses a pump or fan for circulation of fluid. Since active systems require pumps or fans which are operated with electricity, there is additional running costs incurred, making them more expensive compared to passive systems. However, active systems are more effective than passive systems mainly because of high rate of air circulation in the active systems.

2.5.3 Solar Air Heaters (SAHs)

The SAHs are solar systems that transform solar radiant energy into heat, which is transferred convectively from the absorber to the air flowing in the duct. The SAHs occupy an important place among solar heating systems because air is free, non corrosive and can work under all weather conditions without the need for protection against freezing and boiling. This reduces the number of the required system components making SAHs cheap and simple in design as compared to other thermal collectors. The SAHs are better suited for moderate temperature applications where the temperature demand range is 30- 80 ^{0}C. Solar air collectors are generally flat plate collectors. The simplest design of the solar air collector is one with single air flow either above or below the absorber plate. A schematic diagram of a simple flat plate solar air heating collector is illustrated in Fig. 2.3.

Fig. 2.3: Schematic diagram of flat plate solar air heater (Ong, 1995)

Air heaters are usually classified according to the position of air flow with respect to the absorber plate and the number of air flow channels in the solar collector system. The channel can be in some cases above, or below, or on both sides of the absorber plate. The common types of configuration of SAH systems are illustrated in Fig. 2.4 (Ong, 1995; Forson *et. al*, 2003).

Type I is a single channel design with single air flow between top glass and bottom absorber plate, type II is also a single channel design but with air flow between absorber and back insulation (unglazed), type III is similar to type II but with a glazing and type IV is a double channel design with double air flows between top glass and absorber plate and between absorber and bottom plates. This work investigates the thermal performance of type I collector system with a rectangular corrugated absorber plate.

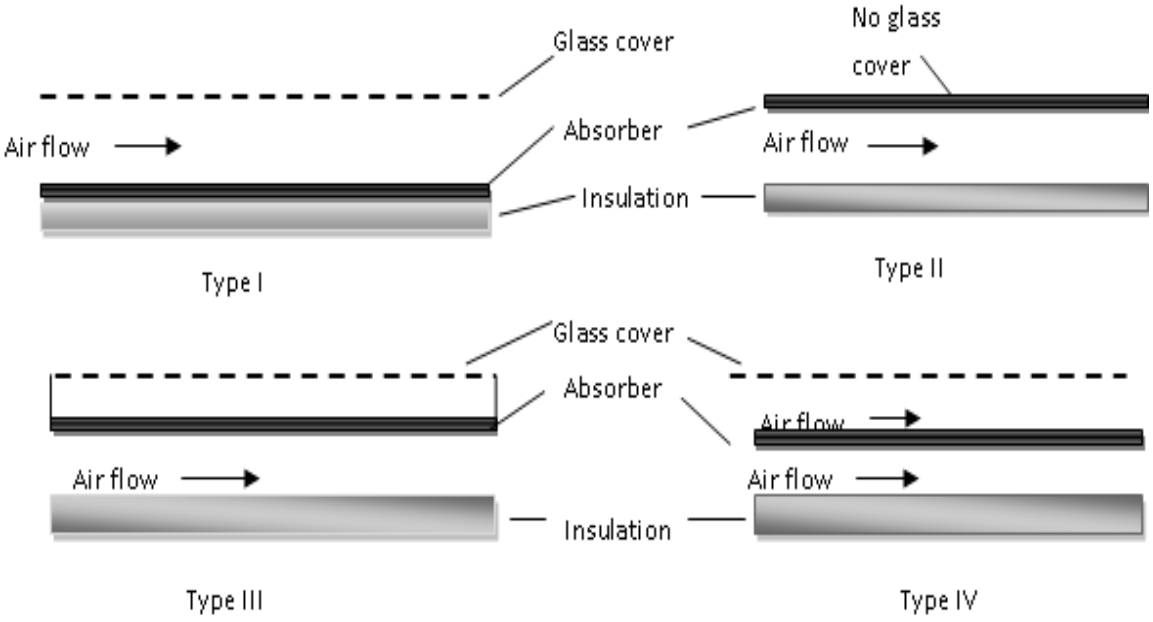

Fig. 2.4: Schematic illustration of different types of solar air collectors (Forson *et. al*, 2003)

The solar air heater systems make use of ambient air as a working fluid for heat removal from the collector and delivering it to the point of application. Several works, both experimental and theoretical, on solar air heaters have been done and published in leading

solar energy journals for over six decades now. Solar air heating technology is still an active research area among the renewable sources of energy since its conversion efficiency is still low and the prospects for improvement are still there. Further, solar air systems are not available in the market because of their bulky nature and their applications being site specific.

The first extensive theoretical analysis on conventional solar air heaters were done by Close (1963) and Whillier (1964). Both studies considered steady state approach and assumed the governing equations of the system to be time independent. They also ignored the effect of thermal capacitance of the system's components. Charters (1971) considered the aspects of flow duct design for solar air heaters. He pointed out that, there is no simple method to optimize the flow duct dimensions on purely technical considerations. A combined technical and economical evaluation should be undertaken for each individual installation using the best cost and available local materials. Further, by studying the design specification for the particular solar air heating device, it should then be possible to arrive at a rational method of assigning the flow duct dimensions.

The main disadvantage of SAH systems is their low efficiency. This is attributed to their poor thermal-physical properties which contribute to low convective heat transfer coefficients between the air flow and the channel walls resulting to low thermal efficiencies of SAH systems. A number of performance improvement methods have been suggested and investigated by several authors and reported. Most of the works concentrate on the methods of enhancing the heat transfer coefficient between the

flowing air and channel walls to increase heat extraction and hence thermal efficiency of the SAH system. Attention has been given on the effects of design and operational parameters. The design parameters include the type of air pass, channel depth, number of glazing and type of absorber plate whereas the operational parameters include the mass flow rate, insolation rate, ambient and inlet temperatures and the wind velocity.

The design of solar collectors has been one of the subjects of many theoretical and experimental investigations. Several configurations of SAHs have been developed in search of a suitable design for different types of applications with an aim of improving their conversion efficiency. The conversion efficiency of SAH system depends on the convective heat transfer coefficient between the air flow and the channel walls. Therefore, the methods of improving thermal efficiency involve the ways of increasing the convective heat transfer coefficient in the channel. Different researchers have proposed the introduction of artificial roughness, use of packings, use of fins, changing the profile of the absorber plate, double flow passages and double glazing as some of the ways of improving the convective heat transfer coefficient.

The artificial roughness has been used in the collector channel to break the viscous sub-layer on the heat transferring surface, which reduces thermal resistance and promotes turbulence in a region close to the rougher surface. The increase in turbulence results to high efficiency of the SAH system. Prasad and Saini (1991) and Bhagoria *et al*. (2002) investigated the effect of relative roughness height and pitch on heat transfer and friction factor in transverse ribs placed on top of the absorber plate. Saini and Saini (1995) did a

parametric analysis on the effect of expanded metal mesh geometry on heat transfer and friction factor. Gupta and Solanki (1997) investigated angle of attack on heat transfer and friction factor in rectangular duct having circular wire ribs on the absorber plate. These studies show that artificial roughness improves the thermal performance of SAH systems compared to the conventional system.

The transfer of heat to air flowing through a packed or porous material is also another technique that has been proposed to improve the efficiency of SAH systems. Choudhury and Garg (1993) carried out a detailed parametric analysis of two different types of packed flow passage solar air heaters and compared their efficiencies with conventional air heater configuration with a single glass cover and air flow beneath the absorber. The first modification is similar to the conventional type but with packed air flow passage. The second modification consists of double glazing with a packed air flow passage above the absorber plate. The packing materials in the first modification are not painted but in second modification they are black-painted. The results show that the use of packings in the airflow channel of the solar air heaters helps in improving efficiency significantly due to the turbulence provided by the packings.

The introduction of fins into the air flow path is also another method that has been proposed to enhance the performance of the thermal collector. The fins improve the effectiveness of the collector by providing augmented heat transfer area and interrupting air flow to create turbulence. The combined effect of the two phenomena results in high heat transfer from the absorbing plate to the flowing air. The experimental and theoretical

results obtained by different researchers show that the highest efficiency is obtained with configuration with fins on both the upper and lower plates (Garg *et al.*, 1989; Garg *et al.*, 1991; Hamdan and Jubram, 1992; Pottler *et al*., 2000).

Satcunanathan and Deonarine (1973) introduced the concept of a two-pass air heater where they investigated experimentally a two pass design with air flow above and below the absorber plate and compared the results with the single pass design. Macedo and Altemani (1978), Ong (1982) and Wijeysundera *et al*. (1982) also carried out studies on single and double pass air heaters. They observed that in both natural and forced flow solar air heater systems, double pass configuration systems perform better than the conventional single pass systems with an efficiency of about 10 to 15 per cent more than the single pass system. Yeh *et al*. (1999) theoretically and experimentally investigated the performance of double pass solar air heater with simultaneous air flow over and under the absorber plate. Hegazy (1999) used a computational approach to develop an optimizing criterion in the performance of the solar air heaters operating with fixed or variable pumping power. The simulation results confirmed that the criterion developed can be used for single pass models which have the airflow either over the absorber plate or on both sides of it.

Garg *et al*. (1984) developed a simple steady state mathematical model to investigate the effect of channel depth of the solar air heater under different designs and flow conditions. The results show that to achieve high efficiency without compromising the outlet temperature and pumping power, the depth of the collector should be optimized with

respect to the effective energy. Choudhury *et al*. (1995) carried out similar studies on the effect of channel depth on system performance and found out that small channel depths gives high thermal efficiency. However, smaller channel depths results in an increase in pressure drop and hence the pumping cost.

The heart of any solar collector is the absorber plate and its main purpose is to absorb the incident solar radiation and convert it into heat as effectively as possible. Several studies on ways of improving the absorptivity of the collector plate have been suggested and studied over the years. The absorber plates are usually painted black using ordinary black paints because black surfaces have high solar absorptivity. However, the black surfaces have high infrared emissivity which results to high thermal losses. For high efficiency solar thermal collectors, the absorber plates need to have high absorptivity and low emissivity in the wavelengths of solar radiation involved. Selective paints that have properties of good absorptivity for the incoming solar radiation (short wavelength) and low emissivity for the reradiated IR radiations (long wavelength radiation) have been developed (Duffie and Beckman, 1991). Studies have shown that selective surface do not improve much the performance of SAH systems as compared to surfaces painted with ordinary black paint (Hachemi, 1999; Choudhury, 2002) hence selective surfaces are not cost effective for solar air collectors. In spite of high prices of selective surfaces, they are widely used in freezing climate to improve the performance of solar water heaters.

The cost of operation of the collector system is entirely determined by the pumping power which is a function of pressure drop. Several investigators have given suggestions

on the design selection criteria to use in obtaining the design features of cost effective SAH system with relatively high efficiency at a predetermined pressure drop (Choudhury, 1988 and Choudhury and Garg, 1991). According to Choudhury *et al*. (1995), the pressure drop determines the cost of operation of the solar air heater since increase pressure drop results in high pumping power hence increase in the running cost.

A simple procedure for changing the fluid velocity and also the strength of forced convection involves adjusting the aspect ratio (channel depth to length ratio) of a rectangular flat plate collector with constant flow rate. The influence of collector aspect ratio on solar thermal collector efficiency has been investigated both experimentally and theoretically. Ho-Ming *et al.* (1999) performed a theoretical investigation on the effect of aspect ratio on the collector efficiency of sheet-and-tube solar fluid heater for constant collector area and constant width between the tubes. The results showed that increasing the collector aspect ratio improves the collector efficiency. However, it was noted that increasing aspect ratio increases the fan power hence high operating cost. Hegazy (2000) did modelling work of a single pass double duct solar air heater. The work showed that the aspect ratio is an important parameter in determining the useful heat gain. His study suggests that for variable flow operation, the optimum aspect ratio should be 0.025 m for both natural and forced convection.

Forson *et al*., (2003) provided a mathematical model to predict the performance of a single pass double duct solar air heater. They used the developed model to investigate the effects of the design and operating variables on the performance of single pass double

duct solar air heater. They also performed the sensitivity analysis and outlined the recommendations for an optimal design configuration for a given air heater aperture that maximizes the air temperature and mass flow rate and minimizes the relative humidity. The model was validated by experimental results obtained from a prototype laboratory model and a full scale field model air heater attached to a commercial crop dryer. The results showed that to achieve the required temperature, mass flow rates and relative humidity of the heated air, a compromise between higher values of collector area, collector aspect ratio and collector length to width ratio in needed. They concluded that, the mass flow rate is the dominant factor in determining the efficiency of a natural convection air heater. Therefore, a careful estimation of the mass flow rate is essential.

Bolaji (2005) developed and evaluated the performance of a box type absorber solar air collector for crop drying. He used the box type absorber with an aim of increasing the heat transfer area exposed to the air flowing through the collector channel in order to achieve high temperature and high efficiency with low friction losses in the system. In his study, he found out that both the efficiency and pressure drop increases with increase in mass flow rate because pressure drop depends on the velocity of air in the collector while the increase in mass flow rate results to increase in the convective heat transfer coefficient and a decrease in collector thermal losses.

Lin *et al.* (2006) carried out a parametric study to investigate the thermal performance of cross-corrugated solar air collectors and compared the performance with that of ordinary flat-plate solar air collector. The cross-corrugated solar air collector had the wavelike

shapes for both the absorbing plate and the bottom plate perpendicular to each other and air flows through the channel between them. Two configuration of this collector were considered. In the first type, the wavelike shape of the absorbing plate is along the flow direction while that of the bottom plate is perpendicular to the flow direction and in the second type, the wavelike shape of the bottom plate is along the flow direction and that of the absorbing plate is perpendicular to the flow direction. They observed that the modified types have a significantly improved thermal performance compared to that of the flat-plate type, with the achievable efficiencies of 55.92%, 57.04% and 40.21% for the first type, second type and flat-plate respectively, under the same operating conditions. They also noted that to achieve higher collector efficiency, it is essential to construct solar air collectors having slender configurations along the air flow direction (length greater that width) because of the monotonic reduction of the convection heat transfer from the absorbing plate to the fluid and the monotonic increases of the thermal radiation heat losses from the absorbing plate to the bottom plate and to the cover when W increases resulting to the decrease in efficiency.

Liu *et al*. (2007) conducted a parametric study on the thermal performance of a solar air collector with a V-groove absorber. The air flows in the channel formed by the V-groove absorber plate and the back flat plate, along the groove. Fudholi et al. (2008) did similar investigation by modifying existing correlations for the two parallel plates with fully developed turbulent flow with one side heated and the other side insulated. The study showed that V-groove collector is 7.4% more efficient than flat plate collectors. These configurations enhance heat transfer rate between the air and the absorber plate by

increasing the heat transfer surface area, which is crucial to the improvement of the thermal performance of a solar air collector.

Yousef *et al.* (2004) developed internet based mathematical simulation program to find the influence of different parameters, such as mass flow rate, flow channel depth and collector length, on the system thermal performance of a solar air collector in Malaysia. The same program was used to simulate the performance of V-grooves solar air systems with and without porous absorber plate (Yousef *et al*., 2007) and flat-plate with and without porous absorber plate (Yousef and Adam, 2008). These studies found out that higher efficiency is obtained at higher mass flow rate through the air heaters and smaller channel depths. In addition, introduction of double pass, porous material and use of V-grooves absorber plate improved the performance of the collector.

Hikmet (2008) performed a comparison of the double-flow solar air collector with and without obstacles theoretically and experimentally. The influence of various parameters, such as the obstacles, the mass flow rate and the level of absorber plates in duct on the energetic and exergetic efficiencies of the SAH were examined, and the significant variables identified. The results show that the double-pass type of the SAHs has an improved thermal and exergetic efficiencies compared to single pass type of SAHs because of the increased heat-transfer area. In addition, the results show that the use of obstacles in the air flow channel of the collector is an efficient method of adapting in air exchanger according to user needs.

Singh and Sharma (2009) did an analytical investigation of thermo-hydraulic performance characteristics of double flow solar air heater having artificially roughened expanded metal mesh on both sides of the absorber plate. They considered the energy equations for heat transfer in two dimensional fully developed fluid flows in order to analyze the thermo-hydraulic performance and to investigate the effect of system parameters such as relative long way length of mesh, relative short way length of mesh, relative height of mesh and operating parameters such as mass flow rate and insolation. They observed that the introduction of an expanded metal mesh artificial roughness on both sides of the absorber plate and allowing equal flow of fluid above and under the absorber plate considerably enhances the thermal performance of the SAH system.

Aharwal *et al.* (2010) investigated the effect of channel width on the heat transfer coefficient and attempted to determine the optimum width of a channel in the inclined rib to form discrete rib for the better heat transfer performance. It was found that inclined rib with relative gap width (g/e) of 1.0 gives the highest value of heat transfer coefficient compared to the other relative gap width. To investigate the effect of gap width on the flow field, a Two Dimensional Particle Image velocimetry (2-D PIV) system was used. The level of turbulence intensity at different relative gap width was measured and observed that the highest value of turbulent intensity is at the relative gap width of 1.0 which is in the line of heat transfer measurements.

Sharma and Varun (2010) carried out an exergy analysis on the performance evaluation of solar air heater having continuous rib as a roughness element on the absorber plate.

From their study, they found out that the exergy efficiency is improved by using roughened geometries in the duct of solar air heater. The exergy efficiency based criterion shows the better results at lower value of Reynolds number but at higher value of Reynolds number, the exergy efficiency becomes negative or exergy of pump work required exceeds the exergy of collected heat energy by solar air heater. They concluded that the exergy analysis yields useful results and provides meaningful criterion for performance evaluation. Also there is no a single roughness geometry which gives best exergetic performance for whole range of Reynolds number. Solar air heater having rib-grooved and arc shaped wire as artificial roughness is found to have better exergy efficiency in the lower range of Reynolds number. However, smooth duct is found suitable in the higher range of Reynolds number.

2.6 Useful Heat Gain in Solar Collector

A simple model describing the useful energy gained by air flowing in the solar air heater can be obtained from the first law of thermodynamics or energy conservation law. The equation gives a linear relationship between the incident solar radiation, I , the optical losses (Q_ρ), the useful heat gained by air (Q_u) and the total heat loss (Q_L) from the collectors as:

$$Q_s = Q_u + Q_L + Q_\rho \tag{2.1}$$

In equation (2.1) the parameter Q_s is the total heat energy intercepted by the collector absorber plate and is given by:

$$Q_s = (\alpha\tau)AI \tag{2.2}$$

Where ($\alpha\tau$) is the absorptivity-transmitivity product, i.e. the product of the absorptance of the absorber plate and transmittance of the glass cover, A is the absorber plate area and I is the plane of array solar radiation incident on the collector.

The optical losses (Q_ρ) are the solar energy reflected from the front glass cover and is given by:

$$Q_\rho = \rho I A \tag{2.3}$$

where ρ is the reflectivity of the glass cover.

Substituting equations (2.2) and (2.3) into equation (2.1) gives:

$$\tau\alpha I A = Q_u + Q_L + \rho I A \tag{2.4}$$

And rearranging equation (2.4), we obtain the useful heat gained as:

$$Q_u = A\ I(\tau\alpha - \rho) - Q_L \tag{2.5}$$

The total thermal loss Q_L from the solar collector is contributed by the three modes of heat transfer and is given by:

$$Q_L = Q_{cond} + Q_{conv} + Q_R \tag{2.6}$$

Where Q_{cond} is rate of heat loss by conduction from absorber plate through the back insulation, Q_{conv} is the rate of heat loss by convection from the glass cover to the surrounding, Q_R is the rate of heat loss by long wave radiation from the glass cover to the sky.

Several correlation equations have been developed to evaluate the total thermal loss Q_L and reported in many published work. The simplest correlation equation for evaluating Q_L is one which assumes that the heat lost from the solar thermal collector is directly proportional to the temperature difference between the hottest components of the system and the ambient temperature. Incidentally, the absorber plate is the hottest component of the solar air heater and the equation that is generally used to evaluate Q_L is given by (Duffie and Beckmann, 1991):

$$Q_L = U_L A\left(T_p - T_a\right) \tag{2.7}$$

The useful heat gained can be evaluated from two equations. The usual equation that is used to evaluate the quantity of heat gained by the airflow in the duct is given as (Duffie and Beckmann, 1991):

$$Q_u = \dot{m} C_p \left(T_{out} - T_{in}\right) \tag{2.8}$$

Where $\dot{m}$ is the air mass flow rate, C_p is the specific heat capacity of air while T_{out} and T_{in} are the air outlet and inlet temperatures respectively (Duffie and Beckmann, 1991).

The second equation that has been used to evaluate the useful heat gain for solar thermal collectors is that constituted by Hottel, Whillier and Bliss, usually referred to as Hottel-Whillier-Bliss equation (HWB) (Duffie and Beckmann, 1991) given by:

$$Q_u = AF_R\left[(\alpha\tau)I - U_L\left(T_{in} - T_a\right)\right] \tag{2.9}$$

Where, F_R is the collector heat removal factor. This is the quantity that relates the actual useful energy gain of the collector to the useful energy gain if the whole collector surface

were at the fluid inlet temperature. The heat removal factor is given by (Duffie and Beckman, 1991):

$$F_R = \frac{\dot{m}C_p\left(T_{out} - T_{in}\right)}{A\left[\alpha\tau I - U_L\left(T_{in} - T_a\right)\right]} \tag{2.10}$$

The measure of the solar air collector performance is the collector thermal efficiency. The thermal efficiency of the collector is calculated from the useful heat gained and the incident solar radiation. It is normally the ratio of the useful heat gain to the incident solar radiation. The mathematical expression for the thermal efficiency is given as (Duffie and Beckmann, 1991):

$$\eta = \frac{Q_u}{AI} \tag{2.11}$$

Combining eqns. (2.9) and (2.11), gives another expression for efficiency given as:

$$\eta = F_R\left(\alpha\tau\right) - \frac{F_R U_L\left(T_{in} - T_a\right)}{I} \tag{2.12}$$

The transmittance-absorptance product in Eqn. (2.12) is based solely on optical properties of the collector materials. The absorptance provides a measure of the fraction of heat absorbed by the collector plate, while the transmissivity gives a measure of the portion of the radiation transmitted through the glazing cover. Therefore, Eqn. (2.12) is normally used for characterization of the spectral absorption characteristics of the solar thermal collector. A graph of η against the values of $\frac{\left(T_{in} - T_a\right)}{I}$ gives a straight line graph. The slope of the graph $(-F_R U_L)$ represents the rate of heat loss from the collector. The y-intercept, $F_R\left(\alpha\tau\right)$, gives the maximum collection efficiency, called the optical efficiency.

This occurs when the fluid inlet temperature equals ambient temperature $(T_{in} = T_a)$. The other point of interest is the intercept with the $\frac{(T_{in} - T_a)}{I}$ axis. This point of operation can be reached when useful energy is no longer removed from the collector, a condition that can happen if fluid flow through the collector stops (stagnation condition). In this case, the optical energy coming in must equal the heat loss, requiring that the temperature of the absorber increase until this balance occurs. This point defines the maximum temperature difference or "stagnation temperature"

2.7 Determination of heat transfer coefficients

The top heat loss is as a result of heat exchange between the glass cover and the sky through convection and radiation. The top loss heat transfer coefficient U_t can be obtained by the expression:

$$U_t = h_w + h_{rp-g} \tag{2.13}$$

Where, h_w is the wind convective heat transfer coefficient at the top cover and has been generally calculated so far from the following empirical correlation suggested by McAdams (1954):

$$h_w = 5.7 + 3.8V \tag{2.14}$$

where, V is the wind velocity and it is usually assumed to be 1.5 m/s (Zhai *et.al*, 2005).

Watmuff *et al*. in 1977 also suggested another correlation given as:

$$h_w = 2.8 + 3.0V \tag{2.15}$$

The radiation heat transfer coefficient, (h_{rg-s}), from the glass cover to the sky is obtained as follows (Zhai *et.al*, 2005).

$$h_{rg-s} = \sigma\varepsilon_g \left(T_g^2 + T_s^2\right)\left(T_g - T_s\right)\frac{\left(T_g - T_s\right)}{\left(T_g - T_a\right)} \tag{2.16}$$

Where, σ is the Stefan–Boltzmann constant, ε_g is the thermal emissivity of the glass cover. The sky temperature, T_s, is estimated by the formulation given by Swinbank (1963) as;

$$T_s = 0.0552 T_a^{1.5} \tag{2.17}$$

The radiation heat coefficient between the absorber plate and glass cover h_{rp-g} is given

$$h_{rp-g} = \frac{\sigma\left(T_p^2 + T_g^2\right)\left(T_p - T_g\right)}{\left(\frac{1}{\varepsilon_p} + \frac{1}{\varepsilon_g} - 1\right)} \tag{2.18}$$

Where ε_p and ε_g are the thermal emissivity of absorber plate and glass cover respectively.

The back heat loss coefficient U_b by conduction through the back insulation is determined by the expression;

$$U_b = \frac{k_i}{d} \tag{2.19}$$

where k_i is the thermal conductivity of the insulation and d is the mean thickness of the insulation.

The natural convection heat transfer coefficient between both the glass cover and the absorber plate and the airflow in the duct is calculated as (Duffie and Beckman, 1991);

$$h_c = Nu \frac{k}{D_h} \tag{2.20}$$

where k is the thermal conductivity of air, Nu is the Nusselt number for the natural convection in the channel formed by the glass cover and the absorbing plate and D_h is the hydraulic diameter of the air flow channel formed by the absorbing plate and the glass cover.

The hydraulic diameter is given by:

$$D_h = \frac{2WL}{(W+L)} \tag{2.21}$$

Where W is the collector width, L is the channel depth.

The Nusselt number can be approximated by the following correlation given by Hollands *et al* (1976)

$$Nu = 1 + 1.44\left[1 - \frac{1708(\sin 1.8\theta)^{1.6}}{Ra\,Cos\,\theta}\right]\left[1 - \frac{1708}{Ra\,Cos\,\theta}\right]^{+} + \left[\left(\frac{Ra\,Cos\,\theta}{5830}\right)^{1/3} - 1\right]^{+} \tag{2.22}$$

Where θ is the angle of inclination of the collector and Ra is the Rayleigh number

$$Ra = \frac{g\beta' \Delta T L^3}{v\alpha} \tag{2.23}$$

Where ΔT, β, and v are the temperature difference between plates, thermal expansion coefficient and kinematic viscosity of air, and g and α is the gravitational constant and thermal diffusivity respectively. The notation $[\ ]^+$ in Eqn. (2.22) is used to denote that if

the quantity in the bracket is negative, it should be set equal to zero. Also, the correlation is valid for $0^o \leq \theta \leq 75^o$.

2.8 Physical properties

The physical properties of air are assumed to vary linearly with temperature, T_f. The following correlation equations were used to determine the physical air properties at the mean air temperature, T_f (Duffie and Beckman, 1991):

Viscosity

$$v = \left[1.983 + 0.00184\left(T_f - 27\right)\right]10^{-5} \tag{2.24}$$

Density

$$\rho = 1.1774 - 0.00359\left(T_f - 27\right) \tag{2.25}$$

Thermal conductivity

$$k = 0.02624 + 0.0000758\left(T_f - 27\right) \tag{2.26}$$

Specific heat capacity

$$C_p = 1.0057 + 0.000066\left(T_f - 27\right) \tag{2.27}$$

CHAPTER THREE

MODELLING METHODOLOGY

3.1 Introduction

This chapter entails the description of the solar air collector under study, the modelling procedure, the energy balance equations of the model and the assumptions made in obtaining them, the method used in solving the equations and the solutions obtained.

3.2 Description of the solar air collector under study

The solar air heater under study consisted of a black painted absorber plate insulated at the bottom and covered by a transparent glass cover on top. The channel between the absorber plate and glass cover forms an open-ended rectangular duct through which air flows. The collector measures 50 cm by 100 cm with the channel depth kept at 15 cm. The collector was installed at an inclined angle of 15^{o} to the horizontal to allow the air to flow by natural convection as shown in Fig. 3.1. The solar energy absorbed by the collector plate heats up the air entering the channel at the ambient temperature (T_a). The air is heated as it flows in the duct from the inlet to the outlet, where its temperature rises from the ambient temperature (T_a) at the bottom to a higher outlet temperature (T_{out}). The glass cover is assumed to uniformly gain heat energy directly by thermal radiation from the absorber plate. The absorber plate is made from the ordinary corrugated roofing iron sheet with trapezoidal profile. The surface of the absorber plate is painted with the ordinary black paint to increase its absorptivity of the incident solar radiation. The plate

is insulated at the back surface with insulating foam to minimize heat losses by conduction.

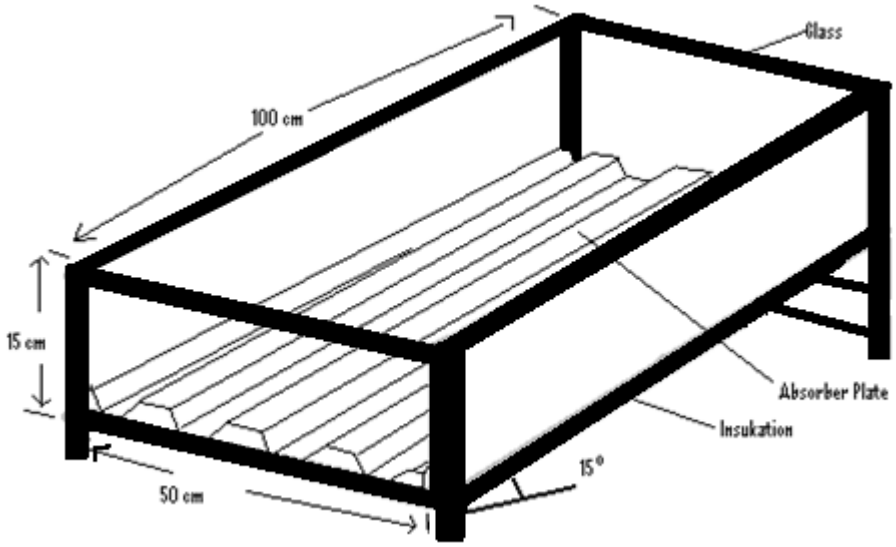

Fig. 3.1: An illustration of the solar air heater under study

3.3 Theoretical modelling

The theoretical studies of the performance of the SAH system involve the formulation of the energy balance equations between the air heater components, the air flow in the channel and the ambient (surrounding). Several assumptions are usually made to ease the thermal analysis of any kind of solar thermal system. The assumptions that were considered in the development of this model are:

1. The air heater operates under steady state conditions.
2. The operating temperatures of the air heater components are constant.
3. The temperature of the air varies linearly along the collector.
4. The air heater is treated as an inclined chimney.

3.4 Energy Balance Equations

The thermal analysis is based on the energy balances that describe the heat transfer mechanisms at each component of the solar air collector. The heat transfer mechanisms are shown in Fig. 3.2. If the rate of solar radiation incident on the glass cover is *I*, then the solar radiation absorbed by the absorbing plate per unit area, *S*, is given as:

$$S = (\tau\alpha)I \tag{3.1}$$

where τ is the transmittance of the glass cover and α is the absorptivity of the absorber plate.

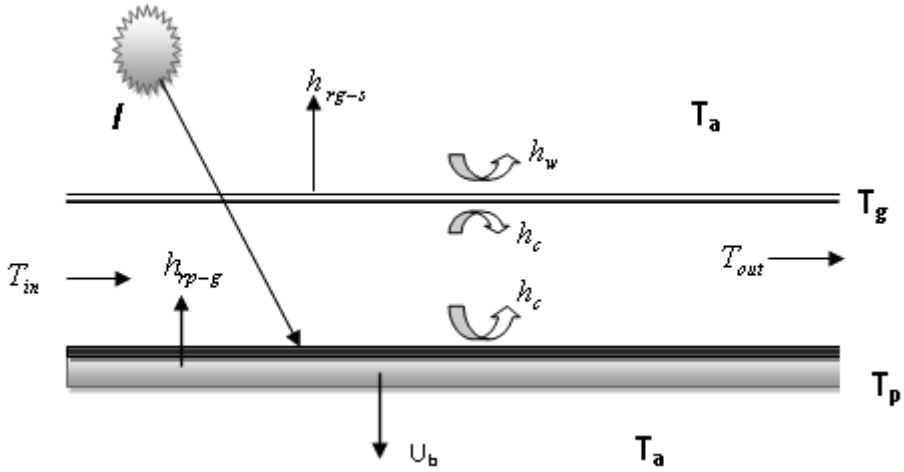

Fig. 3.2: Schematic diagram of the flat plate solar collector with heat transfer parameters

This absorbed energy is distributed to thermal losses through the glass cover, the back and side insulation and to useful energy gain which heats the air in the channel.

On the glass cover, the energy balance equation is given by

$$h_{rp-g}\left(T_p - T_g\right) = U_t\left(T_g - T_a\right) + h_c\left(T_g - T_f\right) \tag{3.2}$$

The term on the left-hand side of eqn. 3.2 gives the heat gained by the glass cover from the absorber plate. The first and second term on the right hand side of equation (3.2) gives the top heat loss from the glass cover to the surrounding and the heat transferred from the glass cover to the flowing air by convection respectively.

On the absorber plate, the absorbed solar radiation, *S*, in eqn. (3.1) is distributed to thermal conduction losses through the back and side insulation, heat exchange between the glass cover and the absorber plate by radiation and heat transfer to the airflow in the duct by convection. Thus, the energy balance equation of the absorber plate becomes;

$$S = h_c\left(T_p - T_f\right) + h_{rp-g}\left(T_p - T_g\right) + U_b\left(T_p - T_a\right) \tag{3.3}$$

The temperature, T_f, in eqns. (3.2) and (3.3) is the mean air temperature in the duct. Assuming linear temperature rise in the duct, T_f is evaluated as the mean of the inlet temperature T_{in} and the outlet temperature T_{out}:

$$T_f = \frac{T_{out} + T_{in}}{2} \tag{3.4}$$

On the air channel, the flowing air receives heat by convection from the absorber plate and the glass cover. The absorbed energy is converted into useful energy resulting to the following energy balance equation:

$$\dot{m}C_p\left(T_{out} - T_{in}\right) = Ah_c\left(T_g - T_f\right) + Ah_c\left(T_p - T_f\right) \tag{3.5}$$

The equations (3.1) to (3.5) are used to derive the solutions for the collector components' temperatures, i.e. T_p, T_g and T_{out} .

The solutions obtained are given as:

$$T_p = \frac{S + h_{rpg}T_g + h_cT_f + U_bT_a}{h_{rpg} + h_c + U_b} \tag{3.6}$$

$$T_g = \frac{h_{rpg}T_p + U_tT_a + h_cT_f}{U_t + h_c + h_{rpg}} \tag{3.7}$$

$$T_{out} = \frac{Ah_c}{\dot{m}C_p}\left[T_p + T_g - 2T_f\right] + T_{in} \tag{3.8}$$

3.5 Theoretical solution procedure

The analytical solutions of the system temperatures T_p and T_g as well as the outlet air temperature, T_{out} are given in Eqns. (3.6), (3.7) and (3.8) respectively. These equations cannot be solved directly because most of the heat transfer coefficients are functions of these temperatures. Hence, an iteration process is involved to solve and obtain the values of plate, glass and outlet temperatures. The iteration process involves the repetitive calculation of a numeric value until the new and the preceding values are equal or very close. In the iteration process, initial first guessed values are assigned to these system temperatures and used to calculate the convective and radiative heat transfer coefficients. The values of the calculated coefficients are then used to determine the new values of T_p, T_g and T_{out}. The newly calculated temperature values are compared with the previously assumed ones. The iterative process is repeated until all the consecutive system temperatures differs by less than 0.01 ^{0}C. The computer program, based on FORTRAN, was developed to perform the iteration process of the solar air collector.

The program starts by asking for the ambient conditions (solar radiation, *I*, and ambient temperature, T_a) as the input parameters. The solar radiation is used to determine the energy flux received by the system whereas the ambient temperature generates the initial guessed values of input temperature, plate temperature, glass temperature and the outlet temperature. The program then considers the configuration parameters (length, *L*, and width, W) from which the collector area is calculated. The program also considers the collector inclination angle, θ, which is used in calculating the Nusselt number and hence the convection heat transfer coefficient. In addition, the program considers the system components characteristics which include plate emissivity, ε_p, glass emissivity, ε_g, plate absorptance, α_p, and conductivity of the back insulation, k_i, that have an effect on the heat losses of the collector system, glass transmittance, τ, and glass absorptance, α_g, which determines the amount of solar radiation intercepted on the collector and conductivity of air, k, the mass flow rate, $\dot{m}$, specific heat capacity of air, C_p, and kinematic viscosity, v, which influences the useful heat absorbed by air.

The program assigns the initial guessed values for absorber plate temperature, T_p, glass temperature, T_g, mean air temperature, T_f, inlet temperature, T_{in}, and outlet temperature, T_{out}, based on the input ambient temperature, T_a. Using the values of solar insolation, the program calculates the energy flux, *S*, intercepted on the plane of collector using Eqn. (3.1). It also calculates the wind heat transfer coefficient, h_w, using Eqn. (2.14). Further the program determines the sky temperature, T_s, using the value of the ambient temperature and Eqn. (2.17). These values are used in the iteration loop where the values of the system temperatures of the model are determined

In the iteration loop, the initial guessed values of the outlet temperature, fluid temperature, glass temperature, sky temperature and plate temperature are used by the program to calculate the top loss heat transfer coefficients, U_t, glass to sky radiation heat transfer coefficients, $h_{rg\text{-}s}$, plate to glass heat transfer coefficients, $h_{rp\text{-}g}$, back insulation heat transfer coefficients, U_b and convection heat transfer coefficients, h_c, using Eqns. (2.13), (2.16), (2.18), (2.19)and (2.20) respectively. The calculated values of the heat transfer coefficients and heat loss coefficients are used to determine new values of the mean air temperature, T_{f1}, the absorber plate temperature, T_{p1}, the glass cover temperature, T_{g1}, and outlet temperature, T_{out1} using Eqns. (3.4), (3.6), (3.7) and (3.8) respectively.

The outlet temperature was used as the control parameter in the model in order to initiate the iteration loop. It is usually chosen as the control parameter in decision making because its value can be varied easily by changing the amount of mass flow rate. The value of the mass flow rate used in the loop will depends on whether the calculated outlet temperature meets the condition used in decision making or not. Normally, If the new value of the outlet temperature is large, then it means that the mass flow rate is low thus the program will add 0.001 to the given value of mass flow rate and the new value is used in the next iteration. On the other hand, if the new value of the outlet temperature is small, then it means that the mass flow rate is high and therefore the program subtracts 0.001 from the given value of mass flow rate and the new value of mass flow rate is used in the next iteration.

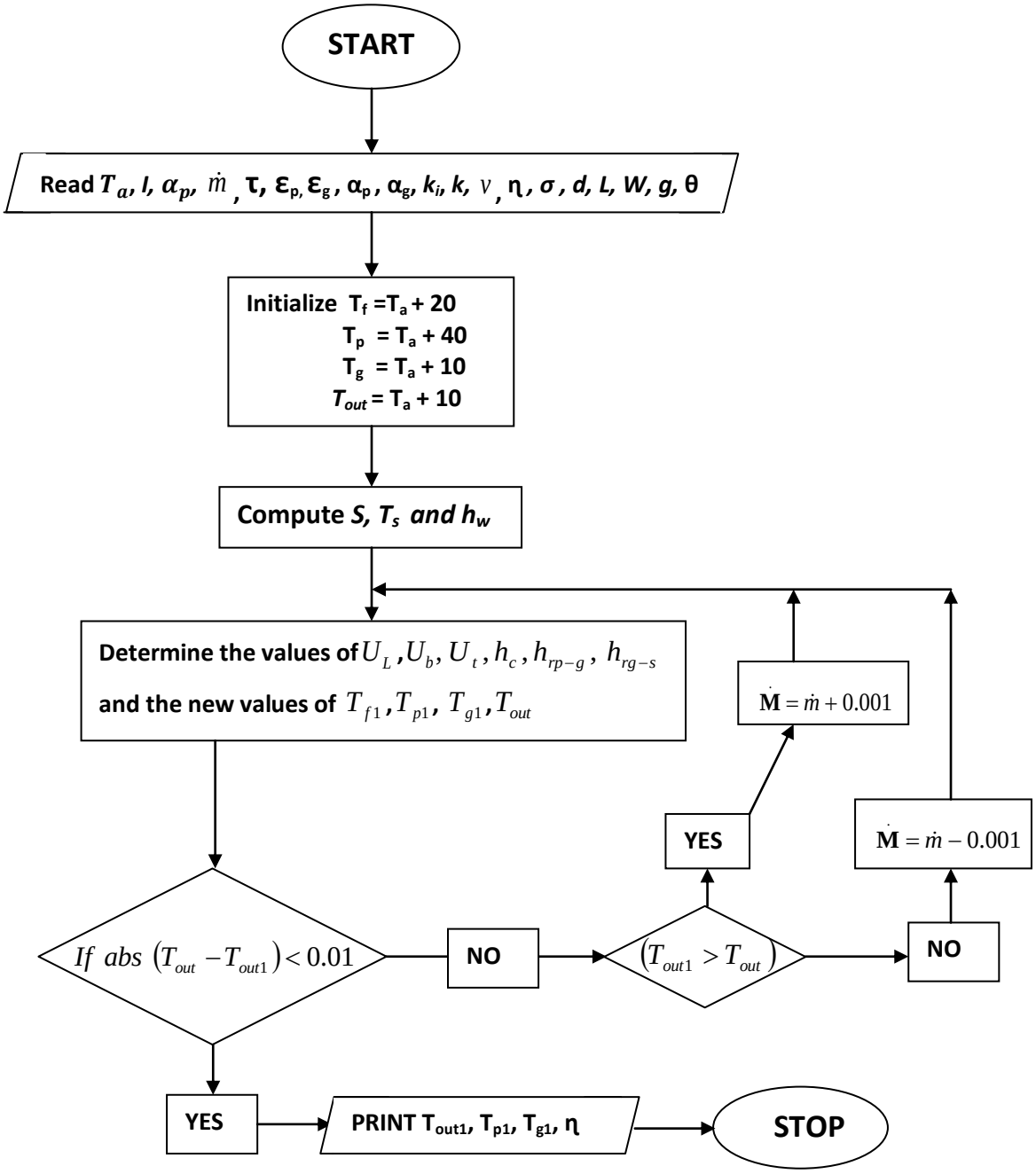

Fig. 3.3: Flow chart for the iterative solution of the mathematical model

The program makes a decision by calculating the difference between the new values of output temperature (T_{out1}) with the previous value (T_{out}). If the absolute value of this temperature difference is greater than 0.01 ^{o}C, then the process is repeated and if it is less or equal to 0.01 ^{0}C then the program exits. The old outlet temperature is then replaced with the newly calculated value and taken to be the required outlet air temperature. The program then proceeds to calculate the efficiency of the system. These results of the calculated outlet temperature, plate temperature, glass temperature and the efficiency are then printed by the program. The flowchart of the computer program used to model and simulate the results of the studied SAH system is as shown in Fig. 3.3.

CHAPTER FOUR

RESULTS AND DISCUSSIONS

4.1 Introduction

This chapter presents the results obtained from the theoretical model, validation results and the analytical results on thermal performance of the solar air heater. The results are presented in graphical form and the numerical data is given in Appendix II.

4.2 Validation of the Model

The validation of the model was done by comparing the predicted and the measured values of the system temperatures. The experimental results were measured on a prototype model built and tested outdoors at the Department of Physics, Moi University (Maritim, 2010).

Fig. 4.1 shows the validation results, where the theoretical and experimental output air temperatures are compared for a selected representative day. The graph shows a plot of temperature against time of the day when the measurements were done. The results show that the theoretical, $T_{o,cal}$ and experimental, $T_{o,exp}$, output air temperatures are almost equal with a small deviation of less than 2.5 ^{o}C. This gives a good correlation between $T_{o,cal}$ and $T_{o,exp}$.

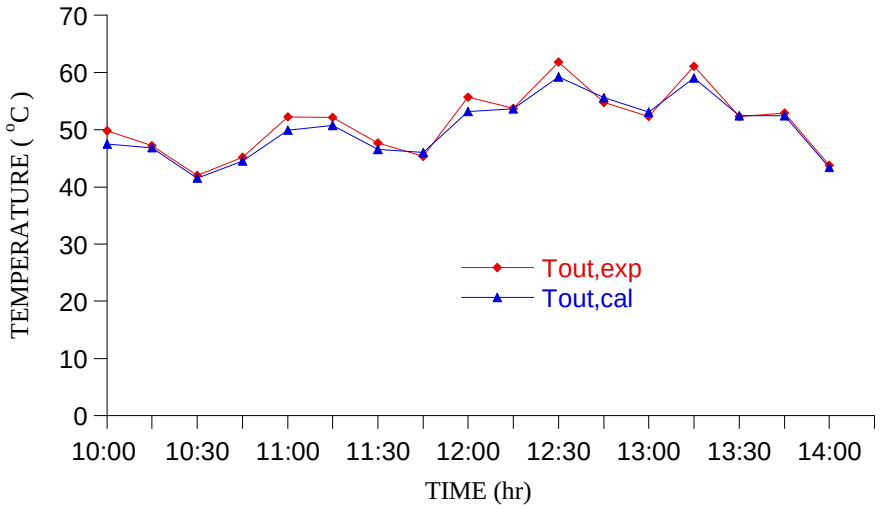

Fig. 4.1: Correlation between the theoretical and experimental output temperature

Fig. 4.2 shows the correlation between the theoretical and experimental values of the plate temperature against time of the day. In order to measure the plate temperature, it is recommended to mount temperature sensors at several points on the absorber plate area to enable the average plate temperature to be obtained. This will give the average plate temperature more accurately but such process is cumbersome. Thus, the plate temperature is usually measured at two locations on the plate. One sensor is placed at ⅓ and the other at ⅔ from the inlet of the collector and their average value is used as the plate temperature. This is how the plate temperature was measured in the experimental model (Maritim, 2010). In Fig. 4.2, the plate temperatures measured at the two locations, T_{p1} and $T_{p2,}$ are plotted together with the theoretical value. The results show that the theoretical values lie symmetrically between the two experimental values (i.e. at the ⅓ and ⅔ positions) and with a similar profile.

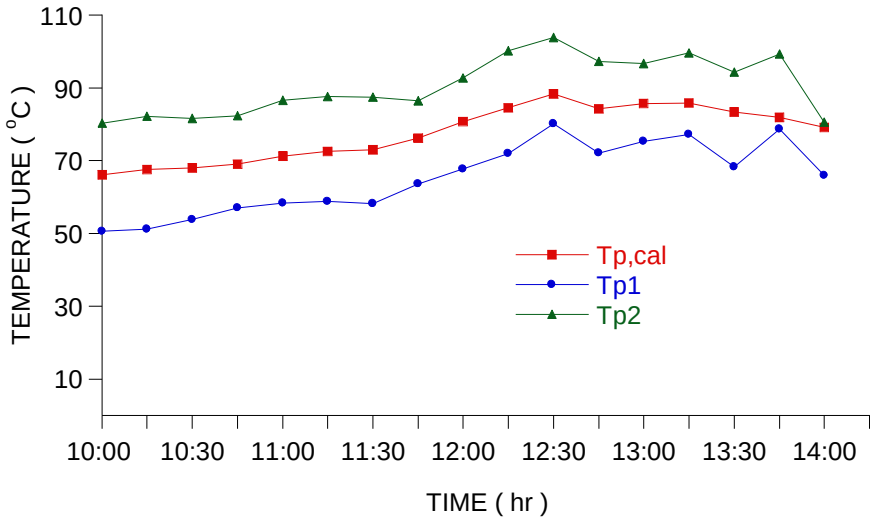

Fig. 4.2: Comparison between the experimental and theoretical plate temperatures

Comparison between the theoretical values and the average of the two plate temperature values is also given in Fig. 4.3. The results show that the calculated and the average experimental values are almost equal throughout the day. In addition, the plate temperature in both cases increases to a maximum value at some time past mid-day when the solar radiation intensity is high and then starts to fall due to the decrease in the solar radiation intensity showing that the plate temperature depends on the amount of solar radiation intercepted on the absorber plate. It is also observed that the fall of the plate temperature does not assume the in-phase response to solar radiation due to the effect of thermal mass. The thermal mass provides 'inertia' against temperature fluctuations resulting to a time lag between system's temperature and solar radiation.

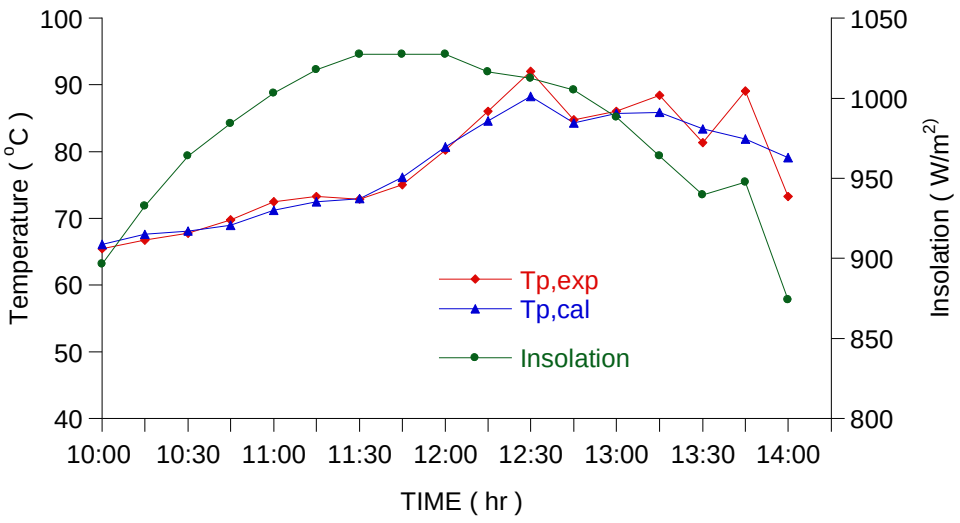

Fig. 4.3: Representation of the trend of insolation and the corresponding correlation between $T_{p,exp}$ and $T_{p,cal}$ of the representative day

4.3 Modelling Results

The model was used to investigate the effect of mass flow rate, solar radiation, ambient temperature, channel depth and the collector length and width on the thermal performance of the SAH.

4.3.1 Effect of Mass Flow Rate

The mass flow rate is one of the major operational parameters that greatly affect the performance of the SAH system. The variation of the mass flow rate influences the rate of exchange of heat energy between the channel walls and the air flowing in it hence the change in efficiency.

The mass flow rate was varied from 0.001 – 0.025 kgs^{-1} and the efficiency of the collector investigated at three different input temperatures. Fig. 4.4 shows the computed values of the efficiencies plotted against the mass flow rate.

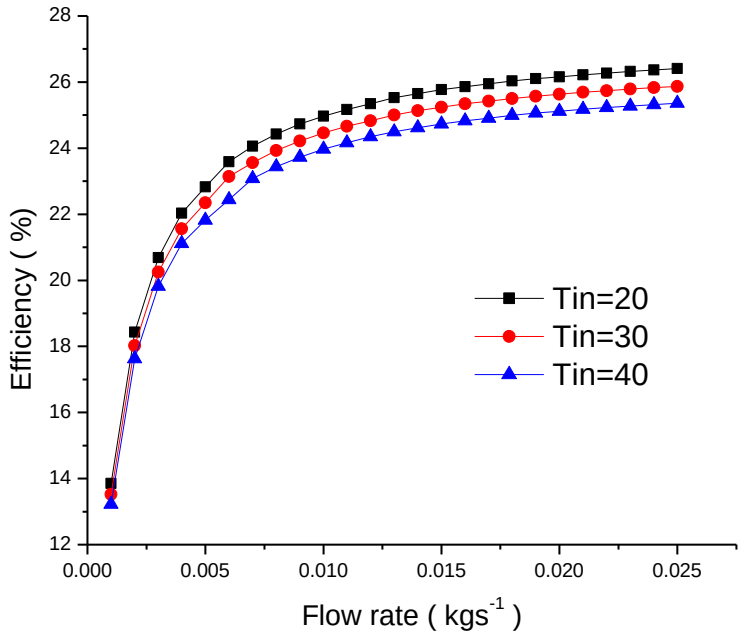

Fig. 4.4: Effect of flow rate on the efficiency at different inlet temperature

It is observed that the efficiency increases with increasing mass flow rate for all input air temperatures. It is also observed that when the mass flow rate is below 0.005 kgs^{-1}, the increase in efficiency of the collector is rapid but thereafter the increase becomes gradual tending to saturate at some point of the mass flow rate. As the mass flow rate increases, the collector operating temperatures are lowered (as presented in Fig. 4.5) since more air flows through the duct absorbing more heat from the absorber plate, the glass cover and side walls of the collector resulting in the increase in collector efficiency. However, as

the flow rate increases, the temperature difference between the output temperature and the inlet temperature decreases resulting to the decay in the increase of the collector efficiency. Further, the results show that the system works more efficiently at relatively low input temperatures because of low heat losses from the system as per Newton's law of cooling.

Fig. 4.5 presents the variation of outlet temperature, plate temperature and glass temperature with the mass flow rate.

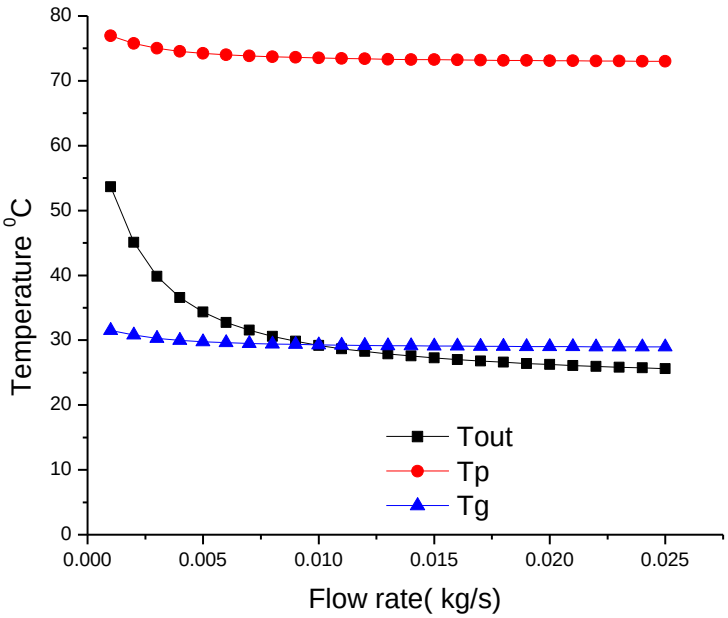

Fig. 4.5: Effect of flow rate on T_p, T_g and T_{out}

The results show that the outlet temperature, the plate temperature and the glass temperature decreases with increase in mass flow rate. However, its effect is greatly

noted on the output temperature than on both the plate and the glass temperatures. As the flow rate increases, the T_{out} decreases exponentially because of the increased airflow velocity in the air channel. The increased velocity make the air spend little time flowing in the channel hence the heat intercepted results in smaller temperature rise as the mass flow rate increases. More interestingly, it is observed that the glass temperature is less than the outlet temperature for mass flow rate below 0.01 kgs^{-1} and thereafter becomes greater than outlet temperature. When $T_{out} > T_g$, the air flow heats the glass cover instead of gaining heat from glass hence representing heat loss mechanism as far as heat production is concerned. Beyond the mass flow rate of 0.01 kgs^{-1}, the air flow gains heat energy from both the glass cover and absorber plate resulting to the gradual increase in thermal efficiency. Therefore, the mass flow rate should be greater than 0.01 kgs^{-1} for the air to gain heat from both the glass cover and absorber plate so as to achieve high efficiencies. Furthermore, a good choice of mass flow rate should be determined depending on the kind of application of the system so as not to compromise the outlet temperature for efficiency since high mass flow rate results to low output temperature.

4.3.2 Effect of solar radiation, *I*, on thermal efficiency

The quantity and intensity of solar radiation intercepted on the absorber plate varies from time to time during the day. These variations affect the thermal performance of the SAH system. The plane of array (POA) solar radiation was varied in the range of 150–1200 W/ m^2 to investigate the effect of solar radiation on the collector thermal efficiency at three different ambient temperatures and also at four different channel depths.

Fig. 4.6 shows the variation of thermal efficiency with POA solar radiation at three different ambient temperatures (20 ^{o}C, 30 ^{o}C and 40 ^{o}C). The results show that efficiency increases with increase in insolation at any given ambient temperature. An increase in solar insolation usually increases the amount of solar energy intercepted on the absorber plate resulting to an increase in plate temperature.

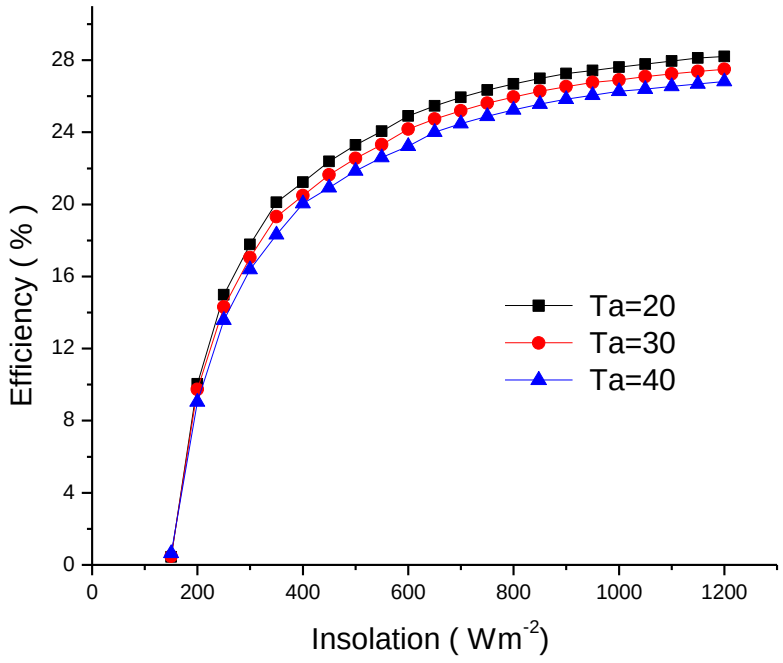

Fig. 4.6: Variation of thermal efficiency with insolation at different ambient temperatures

The rise in the plate temperature results to the increase in the rate of exchange of heat energy between the air flow and the collector walls which leads to increase in the outlet temperature and hence increase in efficiency. It is also observed that the efficiency of the system is zero below the threshold radiation (150 Wm^{-2}). This is the minimum amount of

solar radiation needed to warm the collector system to start producing heat. Further, it is observed that the ambient temperature has little effect on the efficiency of the collector at low solar insolation (below 300 Wm^{-2}). The heat loss from the collector system at low solar insolation is low compared to higher insolation rate. This causes the effect of change of the ambient temperature to be minimal at low insolation rate.

Similarly, the effect of insolation on thermal efficiency of the SAH at different channel depths was investigated and the results are as shown in Fig. 4.7.

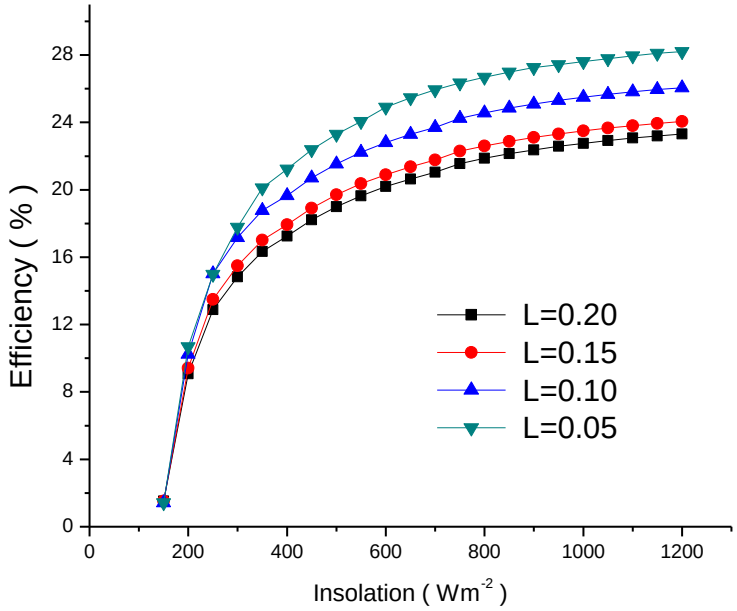

Fig. 4.7: Effect of insolation on efficiency at different channel depth

The results show similar trend to that in Fig. 4.6 whereby the collector efficiency increases with increase in insolation and tends to saturate at higher values of insolation.

In addition, the collector efficiency for smaller channel depths is observed to be higher than for larger channel depths. Smaller channel depths usually have high convective coefficients which lead to higher efficiencies.

The effect of insolation on the air outlet, glass cover and absorber plate temperatures was also investigated. The results obtained are presented in Fig. 4.8. It is observed that the glass cover, the absorbing plate, and the output air temperatures increases almost linearly with increase in the insolation rate. The temperature of the plate is highest showing that it is the hottest component of the collector. Furthermore, the rate of increase of its temperature with insolation is higher than both the glass cover and outlet temperatures because it is well insulated. The linear increase in both the glass cover and airflow temperature may result from linear increase in the heat transfer from the absorbing plate to the glass cover and airflow.

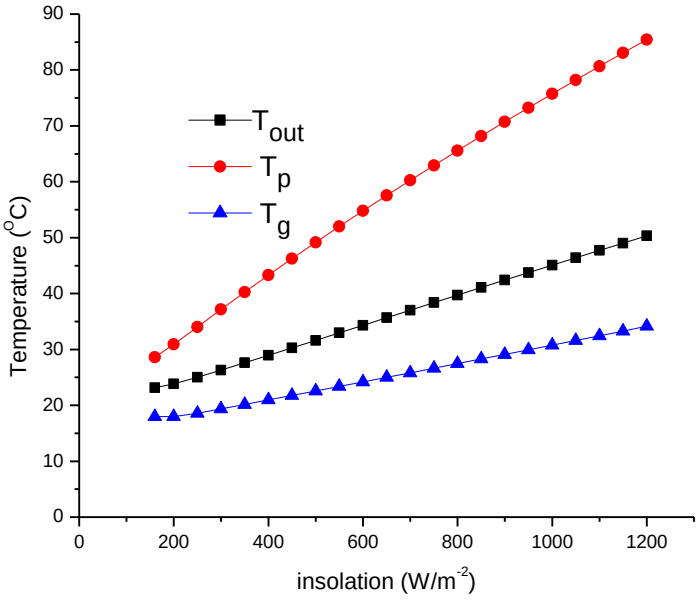

Fig. 4.8: Effect of insolation on the calculated value of T_p, T_{out} and T_g

4.3.3 Effect of Channel Depth

The channel depth is one of the design parameters that determine the performance of the solar air heater. The efficiency of the collector was determined at different ambient temperatures as the channel depth varied from 0.05 – 0.2 m. Fig. 4.9 shows the variation of the efficiency with channel depth for three different ambient temperatures.

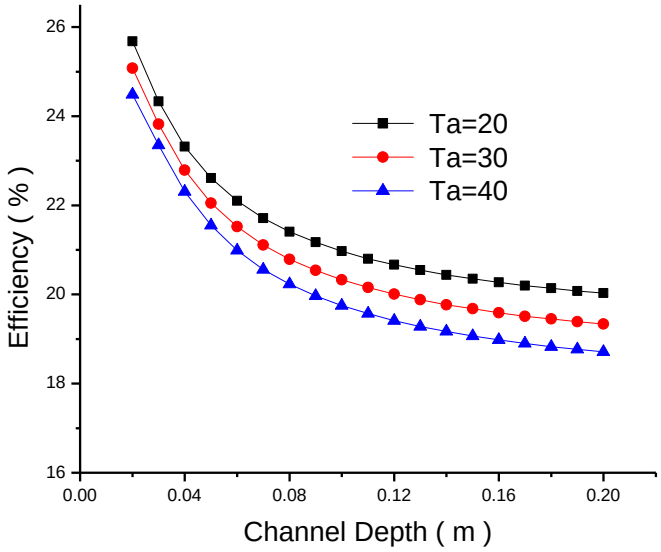

Fig. 4.9: Efficiency against channel depth at different inlet temperature

The results show that the efficiency of the collector decreases with increase in channel depth at all ambient temperatures. In addition, for a given channel depth, the collector efficiency is higher at low ambient temperatures than at high ambient temperature. An increase in the channel depth increases the hydraulic diameter resulting to reduction of the convective heat transfer coefficient hence the efficiency. Therefore, smaller channel

depths can be used for natural flow mode to achieve high efficiencies. However, a decrease in channel depth increases the pressure drop in the collector channel hence need for pumping of air as in the case of forced flow mode systems. The pumping of air results to increase in the cost of operation of the collector due to the additional cost of pumping.

4.3.4 Effect of the collector length and width

The collector dimensions usually define the collector area and influences the mass flow rate and the convective heat transfer of the solar system. Their effect on the performance of the collector was investigated by calculating the thermal efficiencies at different values of collector length and width. The results showing the effect of the collector length is presented in Fig. 4.10. In the graph, the values of efficiency calculated at different ambient temperatures are plotted against the collector length ranging from 0.2 - 2.5 m.

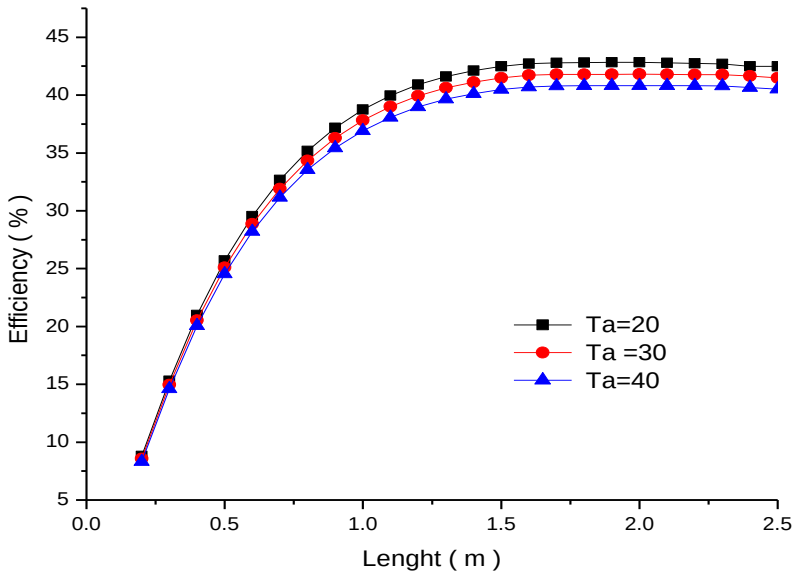

Fig. 4.10: Effect of collector length on efficiency at different inlet temperatures

It is observed that the efficiency at all ambient temperatures increases with increase in the collector length to about 2.0 m and thereafter starts to decrease with further increase in length. The collector area usually determines the total amount of solar radiation that is intercepted by the SAH system. Thus, an increase in the collector length increases the surface area intercepting the solar radiation resulting to higher heat production in the SAH system. It also increases the air residence time inside the solar collector channel and enhances the convective heat transfer rate between the absorber plate and the flowing air (Ho-Ming, 1999). This results to the increase in efficiency as the length increases. Conversely, the increase in collector length results in the increase in pressure drop and thermal losses. The increase in pressure drop is as a result of friction between the air and the channel walls whereas the increase in thermal losses is due to increase in surface area of the collector. The increase in pressure drop and thermal losses leads to a reduction in efficiency when the length exceeds 2.0 m. Therefore, the optimum collector length of the SAH system for optimum efficiency to be achieved should be between 1.5 -2.0 m.

The effect of the variation of the collector width on efficiency is similar to that of the collector length as shown in Fig. 4.11. The variation in the collector width determines the hydraulic diameter and hence the convective heat transfer coefficient. The convective coefficient greatly influences the useful energy gain of the collector. The increase in collector width also leads to increase in the collector area and mass flow rate in the channel resulting to the increase in efficiency. It is observed that the optimum efficiency

is obtained when the width is between 1.0 – 1.5 m. At large collector width, the thermal losses outweigh the absorbed solar radiation causing a decrease in efficiency.

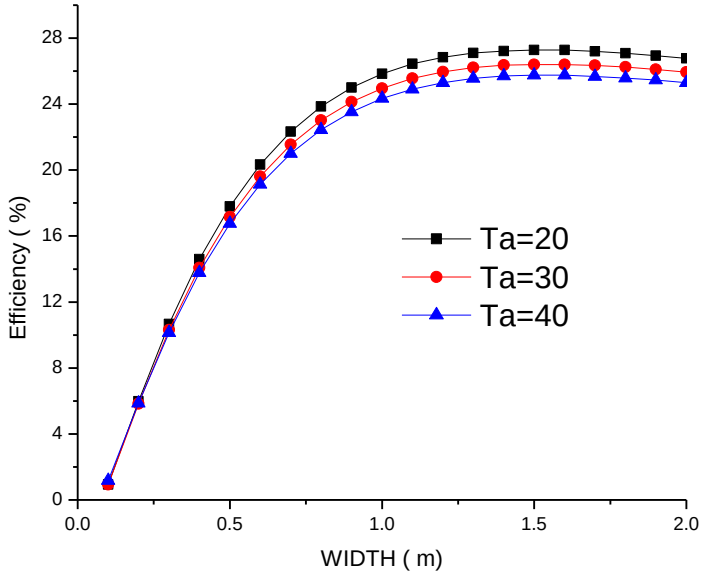

Fig. 4.11: Effect of collector width on efficiency at different inlet temperatures

The two dimensions determine the size of the SAH with the largest being 2 m by 2 m. When constructing a large solar air collector system that is capable of giving the intended outlet temperature (depending on the application) without compromising efficiency, air is often made to flow through several collectors interconnected in either series or parallel or a series-parallel arrangement to form an array. According to Ong (1995) a series only connection would result in a long but higher temperature system whereas a parallel only connection would result in a short but lower temperature system.

4.4 Thermal Performance curves of the Collector

The performance curves of the collector are usually given as a plot of the thermal efficiency of the collector verses the reduced temperature ratio as per HWB equation (2.12). Fig 4.12 presents the theoretical performance curves obtained by plotting the thermal efficiency, η, against reduced temperature ratio, $\frac{(T_{in} - T_a)}{I}$ obtained at different channel depths. The performance equations for these results are given in Table 4.1.

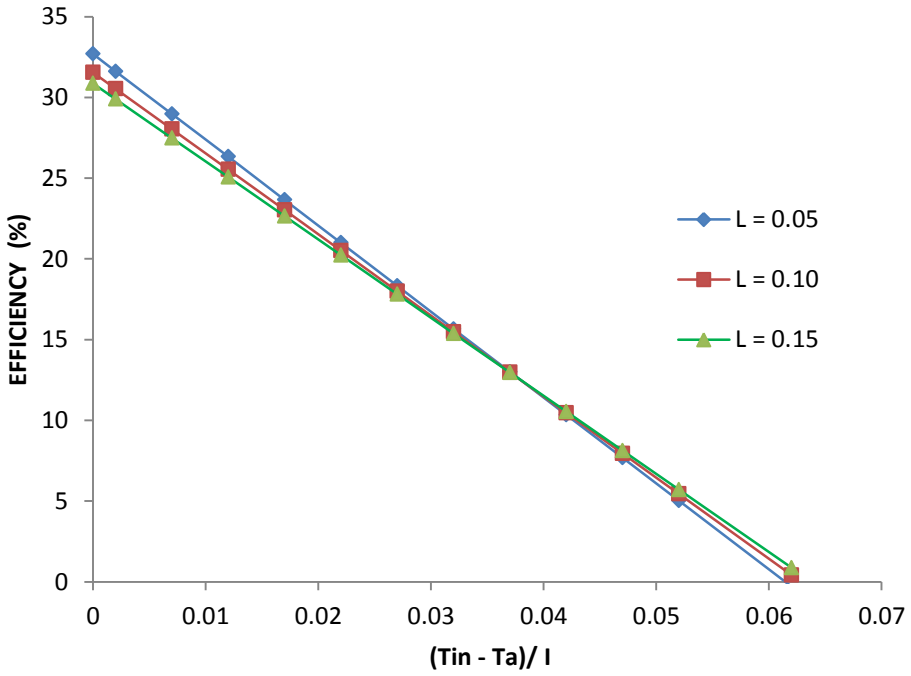

Fig. 4.12: Efficiency against reduced temperature ratio at different channel depth

Table 4.1: Performance Curve equations

Channel depth (m)	Performance curve equations	Maximum Optical efficiency (%)	Temperature difference at stagnation (^oC)	F_R	U_L ($W/m^2 K$)
0.05	$\eta = 32.70 - 532.1\frac{T_{in} - T_a}{I}$	0.3270	61.45	38.47	13.83
0.1	$\eta = 31.55 - 502\frac{T_{in} - T_a}{I}$	0.3155	62.84	37.12	13.52
0.15	$\eta = 30.87 - 483.7\frac{T_{in} - T_a}{I}$	0.3087	63.82	36.32	13.32

The average values of the overall heat loss and the heat removal factor of the collector are 13.56 W/m^2K and 37.30 respectively. The results also show that the collector can attain a maximum efficiency of between 30% to 33% and a maximum temperature difference of between 61^{o}C to 64^{o}C at stagnation state depending on the channel depth used.

CHAPTER FIVE

CONCLUSION AND RECOMMENDATIONS

5.1 Conclusion

The validation results of the model show good agreement between the calculated and experimental values. Therefore, the developed mathematical model can be used with confidence in designing practical solar air heater system.

From the theoretical results obtained from the model, the following conclusion can be made:

1. The efficiency of the collector increases with the mass flow rate at any input temperature. High thermal efficiency of the collector is achieved when air flow gains heat from both the absorber plate and the glass cover. In order for the air flow to gain heat from the two components of the collector, the mass flow rate should be greater than 0.01 kgs^{-1}.
2. Efficiency increases with increase in solar insolation and it tends to saturate at high values of insolation. An increase in solar insolation increases the rate of heat conversion by the absorber plate resulting in the increase in the rate of exchange of heat energy between the air flow and the collector walls hence increase in efficiency. However, the efficiency of the system is zero below the threshold radiation (150 Wm^{-2}) because the collector system is warming up to start producing heat.

3. Better performances of the collector are obtained at low ambient temperatures because of low heat losses from the system at these temperatures.
4. The collector with small channel depth has higher efficiency.
5. The efficiency of the collector increases with increase in both the collector length and width and attains its optimum values of efficiency between 1.0 m to 2.0 m.

5.2 Recommendations

This study has given a parametric analysis of various design and operational parameters and from the results obtained, the following recommendations have been made:

1. The model can be used to size and design a practical solar air heater.
2. The mass flow rate should be kept above 0.01 kgs^{-1} for the collector to perform at higher efficiencies.
3. Practical solar air collectors should have a length or width of between 1.5 - 2.0 m.
4. For natural flow mode, the collector channel depth should be 0.05 m.
5. Demonstrations on the use of SAH systems should be done to equip the users with the information on the potentials and advantages of using SAHs and knowledge of designing and installing systems that are cost effective in energy production and capital cost.
6. Work on forced flow should be done and the results compared with the present work.

REFERENCES

Abdullah M. K and Gatea A. A., (2011). Performance evaluation of a v-groove solar air collector for drying maize (*Zea mays*) in lraq. *African Journal of Agricultural Research* Vol. 6(4), pp. 817-824.

Aharwal, K. R., Gandhi B. K., Saini J. S. (2010). "An experimental investigation of heat transfer and fluid flow in a rectangular duct with inclined discrete ribs." *International Journal of Energy and Environment* **1**: 987-998

Bhagoria, J. L., Saini, J. S. and Solanki, S. C., (2002). "Heat transfer coefficient and friction factor correlations for rectangular solar air heater duct having transverse wedge shaped rib roughness on the absorber plate." *Renewable Energy* **25**: 341-369

Bolaji, B. O., (2005). "Development and performance evaluation of a box-type absorber solar air heater for drying crops." *Journal of food technology* **3**: 595-600.

Charters, W. W. S., (1971). "Some aspects of flow duct design for solar air heater applications." *Solar Energy* **13**: 283-288.

Choudhury, C., (1988). "A corrugated plate solar air heater: trade-offs between efficiency and pressure drop. Report 88-115 ISSN 0332-5571, Institute of physics, University of Oslo, Norway.

Choudhury, C. and Garg, H. P., (1991). "Design analysis of corrugated and flat plate solar air heaters." *Renewable Energy* **1**: 595-607.

Choudhury, C. and Garg, H. P., (1993). "Performance of air heating collectors with packed airflow passage." S*olar* energy **50**: 205 -221.

Choudhury, C., Chauhan, P. M. and Garg, H. P., (1995). "Design curves for conventional solar air heaters." *Renewable energy* **6**: 739-749.

Choudhury, G.M., (2002). "Selective surface for efficient solar thermal conversion." *Bangladesh Renewable Energy Newsletter* **5**: 1-3.

Close, D. J., (1963). "Solar air heaters for low and moderate temperature applications." *Solar Energy* **7**: 117 -124.

Duffie, A.D., and Beckman, W. A., (1991). *Solar Engineering of Thermal processes*. 2nd Ed. New York: Wiley.

Forson, F. K., Nazha, M. A. A., Rajakaruna, H., (2003). "Experimental and simulation studies on a single pass double duct solar air heater." *Energy conversion management* **44**: 1209-1227.

Fudholi, A., K. Sopian, M.Y. Othman, M.H. Ruslan and M.A., (2008). Heat transfer correlation for the v-groove solar collector. Proceedings of the 8th WSEAS International Conference on Simulation, Modeling and Optimization, Sept. 23-25, Santander, Cantabria, Spain, pp: 177-182.

Garg H.P.,and Garg S.N., (1993). "Measurement of solar radiation – Radiations instruments." *Renewable Energy* **3**: 321-333.

Garg, H. P., Datta, G. and Bhargava, A. K., (1984). "Some studies on the flow passage dimension for solar air heating collectors." *Energy Convers.mngt* **24** No 3: 181-184.

Garg, H. P., Datta, G. and Bhargava, A. K., (1989). "Performance studies on a finned air heater." *Energy* **14**: 87-92.

Garg, H. P., Jha, R., Choudhury, C. and Datta, G., (1991). "Theoretical analysis on a new finned type solar air heater." *Energy* **16**: 1231

Gashie, W., (2006).The role of small and medium-scale renewable energy technologies in poverty alleviation, environmental sustainability and economic development in Ethiopia, Nairobi, AFREPREN/FWD and Heinrich Boll Foundation (HBF).

Gatea A. A., (2010). Design, construction and performance evaluation of solar maize dryer. *Journal of Agricultural Biotechnology and Sustainable Development* Vol. **2**(3), pp. 039-046.

Gueymard C.A., (2004). "The sun's total and spectral irradiance for solar energy applications and solar radiation models." *Solar Energy* **76**:423–453.

Gupta, D., Solanki, S.C. (1997) . "Thermo-hydraulic performance of solar air heaters with roughened absorber plate." *Sol Energy* **61**: 33-42.

Hachemi, A,. (1999). "Theoretical and experimental study of efficiency factor, heat transfer and thermal heat loss coefficients in solar air collectors with selective and nonselective absorbers." *International journal of energy research* **23**: 675-682.

Hamdan, M. A. and Jubram, B. A., (1992) "Thermal performance of three types of solar air collectors for the Jordanian climate." *Energy* **17**: 173-175.

Hegazy, A. A., (1999). "Optimizing the thermo-hydraulic performance of flat plate solar air heaters operating with fixed/variable pumping power." *Renewable energy* **18**: 283-304.

Hegazy, A. A., (2000) "Performance of flat plate solar air heaters with optimum channel geometry for constant/variable flow operation." *Energy conversion management* **41**: 401-17.

Hikmet E., (2008). "Experimental energy and exergy analysis of a double-flow solar air heater having different obstacles on absorber plates." *Building and Environment* **43**: 1046–1054.

Hollands K.G.T., Unny T. E., Raithby G.D., Konicek L.J., (1976. "Free convection heat transfer across inclined air layers." Transactions of the ASME, *Journal of Heat Transfer* **98**:189–193.

Ho-Ming Y., Chii D. H., and Chun H. C., (1999). "The effect of collector aspect ratio on the collector efficiency of sheet and tube solar fluid heaters." *Tam-Kang journal of science and engineering* **2**: 61-68

International Energy Agency (IEA) (2001). *Answers to Ten Frequently Asked Questions about Bioenergy, Carbon Sinks and Their Role in Global Climate Change.* International Energy Agency, IEA Biomass Task 38, Greenhouse Gas Balances of Biomass and Bio-energy Systems, Paris France (http://www.ieabioenergy-task38.org/publications/faq/),

IPCC. (2001). "*Climate Change2001: Mitigation*." Contribution of Working Group III to the Third Assessment Report of the Intergovernmental Panel on Climate Change, B. Metz *et al*. (Eds.), Cambridge University Press, UK.

IPCC, (2010). Climate Change 2007: Synthesis Report, http://www.ipcc.ch/pdf/assessmentreport/ar4/syr/ar4syr/.pdf, retrieved on April 17.

Josie Garthwaite for *National Geographic News* Published March 16, 2011

Kalogirou, S. A., (2004). "Solar thermal collectors and applications." *Progress in energy and combustion science* **30**: 231-295.

Karekezi, S., (2002). "Renewables in Africa – Meeting the Energy Needs of the Poor", Energy Policy. Special Issue – Africa: Improving Modern Energy Service for the Poor, Oxford, Elsevier Ltd **30**: 11-12.

Karekezi, S., and Ranja, T. (1997). *Renewable Energy Technologies in Africa*. London: Zed Books Ltd.

Karekezi, S., Kithyoma, W., Wangeci, J., Gashie, W., Turyahabwe, E., Onguru, O., Balla, P. and Ochieng, X., (2006). The Potential of Small and Medium-Scale Renewables in Poverty Reduction in Africa, Nairobi, AFREPREN/FWD and Heinrich Boll Foundation (HBF).

Kurtbas, I. and Turgut, E., (2006). "Experimental investigation of solar air heater with free and fixed fins: efficiency and energy loss." *Int. J. Sci. Technol*. **1**: 75-82.

IEA, (2004). World Energy Outlook 2004. "World Alternative Policy Scenario"

World Nuclear Association, Nuclear power in France. retrieved 12th April 2011 – *(www.world-nuclear.org/info /inf40.html).*

Lin, W., Gao, W. and Liu T., (2006). "A parametric study on the thermal performance of cross-corrugated solar air collectors."*Applied Thermal Engineering* **26** (2006): 1043–1053.

Liu, T., Lin, W., Gao W., Luo, C., Li, M., Zheng Q., Xia C., (2007). "A Parametric Study on the Thermal Performance of a Solar Air Collector with a V-Groove Absorber." I*nternational Journal of Green Energy* **4** : 601 – 622.

Macedo, I. C., Altemani, A. C., (1978). "Experimental evaluation of natural convection solar air heaters." *Solar Energy* **20**: 367-369.

Maritim, J. K., (2010). "A proto-type solar air thermal collector." Msc. Thesis. Moi University, Eldoret,.

Maser M., (2009). Tidal Energy- a primer. *Blue Energy Canada Inc*.

Matuska T., Zmrhal V., Metzger J., (2009). *Detailed modelling of solar flat-plate collectors with design tool Kolektor 2.2: Eleventh International IBPSA Conference*. Glasgow: Scotland

McAdams W. H., (1954). *Heat Transmission*. 3rd Ed. McGraw-Hill: New York.

Muguti, E., (2001). 'Solar Water Heater Technology', AFREPREN Occasional Paper 10: Renewable Energy Technologies in Africa – An Energy Training Course Handbook, Nairobi, AFREPREN.

Norton, B., (1992). *Solar energy thermal technology*. Springer-Verlag, Heidelburg, Germany.

Ong, K. S., (1982). "Results of investigation into forced and natural convection solar air heater and crop driers." *Reg J Energy Heat Mass Transfer* **4**: 29-45.

Ong, K. S., (1995). "Thermal performance of solar air heaters: mathematical model and solution procedure." *Solar Energy* **55**: 93-109.

Pottler, K., Sippel, C.M., Beck, A. and Fricke, J., (2000). "Optimized finned absorber geometries for solar air heating collectors." *Solar Energy* **67**: 35-52.

Prasad, B. N. and Saini, J. S., (1991). "Optimal thermohydraulic performance of artificially roughened solar air heaters." *Solar Energy* **47**: 91-96.

Saini R. P. and Saini J. S., (1995). "Heat transfer and friction factor co-relations for artificially roughness ducts with expanded metal mesh as roughness elements." *Int. J. Heat Mass Transfer* **40**: 973-981.

Sarkar, M. A. R. and Obaidullah, M., (2006). "Solar Thermal Applications" *Short Course on Renewable Energy Technology*, Bangladesh University of Engineering and Technology, Bangladesh, 17-20

Satcunanathan S. and Deonarine S., (1973). "A two-pass solar air heater" *Solar Energy* **15**: 41-42.

Sharma, M. and Varun. (2010). "Performance estimation of artificially roughened solar airheater duct provided with continuous ribs." *International Journal of Energy and Environment* **1**: 897-910.

Singh, K.D.P. and Sharma, S.P., (2009). "Analytical Investigations on Thermal Performance of Artificially Roughened Double Flow Solar Air Heater." *Ariser* **5**: 1-7.

Smeets, E., and Faaij, A., (2007). "Bio-energy Potentials from Forestry in 2050: An Assessment of the Drivers that Determine the Potentials." *Climatic Change forthcoming*.

Swinbank W.C., (1963). "Long-wave radiation from clear skies."*Quarterly Journal of the Royal Meteorological Society* **89**: 339.

The Concise Columbia Electronic Encyclopaedia, Third Edition. Columbia University Press, Encyclopaedia, 1994.

U.S Congress, Office of Technology Assessment., (1992). *Fuelling Development*: *Energy Technologies for Developing Countries,* OTA-E-516 (Washington, DC: US. Government printing office, April 1992).

Whillier, A., (1964). "Performance of black painted solar air heaters of conventional design." *Solar Energy* **8**: 31.

Wijeysundera, N. E., Lee, A. H., Tijoe, L. E., (1982). "Thermal performance study of two-pass solar air heaters." *Solar Energy* **28**: 363-370.

Wikipedia, the free encyclopedia, *deepwater horizon oil spill*, December 2010-*www*.en.*wikipedia*.org/*wiki/Deepwater_Horizon_oil_spill*.

Yeh, H. M., Y., H.M., Ho C. D., and Hou, J. Z., (1999). "The improvement of collector efficiency in solar air heaters by simultaneously air flow over and under the absorbing plate." *Energy* **24**: 857-570.

Yousef, B. A. A., Adam, N. M., Sopian, K., Zaharim, A., Alghoul, M., (2007). "Analysis of Single and Double Passes V-Grooves Solar Collector With and Without Porous Media." *International journal of energy and environment* **1**:109-114.

Yousef, B. A. A., Adam, N. M., Daud, M., Omar, H., Ahmed, M. H. M. and Musa, A. E., (2004). "Expert System Based Prediction of the Performance of Solar Air in Malaysia."*Journal of Energy and Environment* **3**: 91-101.

Yousef, B.A.A., Adam N., (2008). "Performance analysis for flat plate collector with and without porous media." *Journal of Energy in Southern Africa* **19**: 32-42.

Zhai X. Q., Dai Y.J., Wang R.Z., (2005). "Comparison of heating and natural ventilation in a solar house induced by two roof solar collectors." *Applied Thermal Engineering* **25**:741–757

APPENDICES

Appendix I: The FORTRAN Programming Code

```
.....
! DEFINATION OF TERMS THAT ARE USED IN THE PROGRAM
!Ta              ambient temperature
!Tp              plate temperature
!Tg              glass temperature
!Tf              fluid temperature
!Ts              sky temperature
!Tin             inlet temperature
!Tout            output temperature
!K               thermal conductivity
!U               viscosity
!P               density
!Cp              specific heat capacity
!I               solar insolation
!V               velocity of wind
!P1              steffan boltzman constant
!Eg              glass emmittance
!Ep              plate emmittance
!hw              wind heat transfer coefficient
!hrg             glass sky heat transfer coefficient
!hrpg            plate glass radiation coefficient
!hc              convection heat transfer coefficient
!Ub              insulation coefficient
!g               gravitational accelaration
!B               volumetric coefficient of expansion
!Nu              nusselt number
!Ra              Rayleigh number
!Q               angle of inclination
!Ut               top loss coefficient
!X               absorptivity
!M               mass flow rate
!S               solar radiation on the absober plate
!.....
PROGRAM OUTPUT
IMPLICIT NONE
REAL, PARAMETER::Xg=0.06,Xp=0.9,t=0.9,v=1.5,Eg=0.85,Ep=0.9,p=5.67E-8
REAL,  PARAMETER::  Pr=0.70,V1=1.88E-5,L=0.2,g=9.81,PI=3.412,Q=15,  K=0.029,
D=0.025,
REAL, PARAMETER:: Cp=1008,A=0.5,Ki=0.0519
REAL                    ::S,hrpg,hrgs,hw,hc,Ub,Ut,Ul,F,F1,Dc,FR,Qu
REAL                    ::Ra,B,J,M1,Nu,Tg1,n,I,M
```

```
REAL                ::Ta,Tp,Tg,Tin,Tout,Tf,Ts,Tp1,Tout1
INTEGER             ::Y, COUNT
WRITE (*,*) 'ENTER VALUES OF I, Ta'
READ (*,*)I, Ta
Ta= Ta + 273
Tp = Ta + 60
Tg = Ta + 20
Tin= Ta + 5
Tout = Ta+30
M=0.002
S = (t*Xp)*A*I                      !radiation fluxes
hw = 5.7 + 3.8*V                    !determining of wind transfer coefficient
!hw = 2.8 + 3.0*V
Ts = 0.0552*Ta**(1.5/1)             !determining of sky temperature
DO Y=1,10
 COUNT=0+Y
 hrpg = P*(Tp**2+Tg**2)*(Tp+Tg)/(1/Ep+1/Eg-1)          !plate glass radiation
coefficient
 hrgs = P*Eg*(Tg**2+Ts**2)*(Tg+Ts)*(Tg-Ts)/(Tg-Ta)     !glass sky radiation
coefficient
 B =1/(0.5*(Tp+Tg))
 Ra=g*B*(Tp-Tg)*L**3*Pr/V1**2
 J = 1- (1708/(Ra*cos(Q*PI/180)))                      !changing the value of Q
from
                                                       !degrees to radians
 M1 = ((Ra*cos(Q*PI/180)/5830)**(1.0/3)) - 1
          if (J>0 ) then
             J=J
               else
                 J=0
                  end if
            if (M1>0)then
                M1=M1
                 else
                M1=0
             end if
Nu =1 + 1.44*(1-(1708*(SIN(1.8*Q*PI/180))**(1.6/1))/Ra*cos(Q*PI/180))*J + M1
         hc = Nu*k/L                                   !plate fluid convection
coefficient
          Ub=ki/D
         Ut = hw + hrgs
Ul=((Ub+Ut)*(hrpg*hc+hc*hrpg+hc*hc)+(Ub*Ut*(hc+hc)))/(hrpg*hc+hc*Ut+hc*hrpg+
hc*hc)
 F = (hrpg*hc+hc*Ut+hc*hrpg+hc*hc)/((Ut+hrpg+hc)*(Ub+hc+hrpg)-hrpg**2)
 Dc=M*Cp/(A*Ul*F)                                      ! dimensionless capacitance
 F1=Dc*(1-EXP(-(1/Dc)))
```

```
 FR=F*F1
Qu=A*FR*(S-Ul*(Tin-Ta                                   !useful heat
Tout1=Tin+Qu/(M*Cp)                                     !output temperature
 Tf =(Tout1 + Tin)/2                                    ! fluid temperature
Tg1=(hrpg*Tp+Ut*Ta+hc*Tf)/(Ut+hrpg+hc)
 Tp1=(S+hrpg*Tg+hc*Tf+Ub*Ta)/(hrpg+hc+Ub)
      IF (Tout1>Tout)  THEN
        M=M+0.0001
         ELSE IF (Tout1<Tout) THEN
           M=M-0.0001
         Else IF (ABS(Tout1-Tout)<0.1)then
           M=M
        end if
         Tout=Tout1
        END DO
          n= Qu*100/(A*I)
          ! n = (100*M*Cp*(Tout1-Tin))/(A*I)              !efficiency
write (*,*)'count         :',count
write (*,*)'M             :',M
write (*,*)'Tf            :',Tf-273
write (*,*)'Tg            :',Tg1-273
write (*,*)'Tp            :',Tp1-273
write (*,*)'Tout          :',Tout1-273
write (*,*)'Efficiency n:',n
END PROGRAM OUTPUT
```

Appendix II: Tables of Results

Table B1: The validation results

Time	Insolation W/m^2	T_a (^{0}C)	T_{in} (^{0}C)	T_{p1} (^{0}C)	T_{p2} (^{0}C)	$T_{out, exp}$ (^{0}C)	$T_{p, exp}$ (^{0}C)	$T_{out, cal}$ (^{0}C)	$T_{p, cal}$ (^{0}C)
10:00	896.40	15.90	19.60	50.60	80.40	49.80	65.50	47.50	66.10
10:15	932.85	13.80	19.20	51.20	82.20	47.20	66.70	46.80	67.60
10:30	963.90	13.00	17.90	53.90	81.60	42.00	67.75	41.50	68.10
10:45	984.15	12.00	15.70	57.10	82.40	45.20	69.75	44.50	69.00
11:00	1003.05	12.30	12.60	58.30	86.60	52.20	72.45	49.90	71.20
11:15	1017.90	15.80	17.70	58.80	87.70	52.10	73.25	50.80	72.50
11:30	1027.35	13.70	14.00	58.20	87.50	47.70	72.85	46.60	73.00
11:45	1027.35	12.70	14.10	63.60	86.50	45.30	75.05	46.00	76.20
12:00	1027.35	17.30	22.60	67.70	92.80	55.70	80.25	53.20	80.70
12:15	1016.55	20.90	24.30	72.00	100.20	53.70	86.10	53.60	84.60
12:30	1012.50	20.80	28.60	80.20	103.90	61.80	92.05	59.20	88.30
12:45	1005.25	23.30	25.90	72.20	97.30	54.80	84.75	55.60	84.30
13:00	988.20	23.10	27.40	75.40	96.80	52.30	86.10	53.10	85.70
13:15	963.90	26.50	30.00	77.30	99.60	61.10	88.45	59.00	85.90
13:30	939.60	25.90	29.90	68.30	94.40	52.30	81.35	52.40	83.40
13:45	947.70	25.00	30.20	78.70	99.40	52.90	89.05	52.40	81.90
14:00	874.30	23.60	28.60	66.00	80.60	43.80	73.30	43.40	79.10

Table B2: Effect of mass flow rate on system temperature and efficiency

Flow rate (Kg/s)	System temperature (^{0}C)			Efficiency, η, at different inlet temperature (^{0}C)		
	T_{out}	T_p	T_g	20	30	40
0.001	53.66	76.96	31.50	13.85	13.52	13.22
0.002	45.07	75.75	30.79	18.43	18.02	17.63
0.003	39.86	75.02	30.29	20.69	20.25	19.82
0.004	36.58	74.56	29.98	22.03	21.56	21.11
0.005	34.35	74.25	29.77	22.63	22.15	21.68
0.006	32.73	74.01	29.61	23.59	23.14	22.34
0.007	31.53	73.85	29.51	24.06	23.56	23.08
0.008	30.58	73.72	29.42	24.43	23.93	23.44
0.009	29.82	73.61	29.34	24.73	24.22	23.73
0.010	29.20	73.52	29.29	24.97	24.46	23.97
0.011	28.68	73.45	29.24	25.17	24.66	24.16
0.012	28.25	73.39	29.20	25.34	24.83	24.35
0.013	27.87	73.33	29.16	25.53	25.00	24.50
0.014	27.55	73.29	29.13	25.65	25.13	24.62
0.015	27.26	73.25	29.10	25.77	25.24	24.73
0.016	27.01	73.21	29.08	25.86	25.34	24.83
0.017	26.79	73.18	29.06	25.95	25.42	24.91
0.018	26.59	73.15	29.04	26.03	25.50	24.99
0.019	26.41	73. 13	29.02	26.10	25.57	25.06
0.020	26.24	73.11	29.01	26.16	25.63	25.12
0.021	26.10	73.08	28.99	26.22	25.69	25.18
0.022	25.96	73.07	28.98	26.27	25.74	25.23
0.023	25.84	73.05	28.97	26.32	25.79	25.27
0.024	25.72	73.03	28.96	26.37	25.83	25.32
0.025	25.62	73.02	28.95	26.41	25.87	25.36

Table B3: Effect of Insolation on system temperatures and efficiency at different ambient temperatures and channel depths

Radiation W/m^2	η							System temperatures		
	Ambient temperature, T_a (^{0}C)			Channel depth (m)						
	20	30	40	0.15	0.10	0.05	0.20	T_{out}	T_p	T_g
150	0.44	0.48	0.65	01.53	01.53	01.42	01.42	23.17	28.61	18.00
200	10.04	09.74	09.04	09.07	09.42	10.24	10.68	23.86	30.91	18.00
250	14.99	14.31	13.58	12.88	13.50	15.02	14.99	25.02	34.02	18.57
300	17.77	17.05	16.39	14.83	15.49	17.16	17.77	26.31	37.18	19.37
350	20.11	19.31	18.32	16.34	17.02	18.77	20.11	27.61	40.26	20.17
400	21.23	20.49	20.05	17.26	17.93	19.66	21.23	28.95	43.28	20.97
450	22.38	21.64	20.93	18.22	18.91	20.70	22.38	30.29	46.24	21.78
500	23.30	22.56	21.85	19.00	19.70	21.54	23.30	31.63	49.14	22.58
550	24.05	23.31	22.60	19.64	20.36	22.23	24.05	32.98	51.99	23.39
600	24.91	24.18	23.23	20.19	20.90	22.80	24.91	34.33	54.80	24.20
650	25.47	24.73	24.01	20.64	21.37	23.29	25.47	35.68	57.55	25.01
700	25.94	25.20	24.49	21.05	21.77	23.70	25.94	37.03	60.27	25.83
750	26.34	25.61	24.89	21.56	22.30	24.25	26.34	38.38	62.94	26.65
800	26.69	25.96	25.25	21.87	22.60	24.57	26.69	39.73	65.58	27.47
850	26.99	26.27	25.56	22.14	22.87	24.85	26.99	41.07	68.17	28.29
900	27.26	26.53	25.83	22.37	23.11	25.09	27.26	42.41	70.73	29.12
950	27.42	26.77	26.06	22.58	23.32	25.31	27.42	43.74	73.26	29.95
1000	27.62	26.91	26.27	22.76	23.50	25.50	27.62	45.07	75.75	30.79
1050	27.79	27.09	26.39	22.92	23.67	25.67	27.79	46.40	78.22	31.62
1100	27.95	27.24	26.55	23.07	23.81	25.82	27.95	47.72	80.65	32.46
1150	28.12	27.38	26.69	23.19	23.94	25.95	28.10	49.03	83.05	33.30
1200	28.20	27.49	26.81	23.31	24.05	26.06	28.20	50.34	85.42	34.15

Table B4: Effect of Channel depth on efficiency

Channel depth (m)	Efficiency, η, at different Ambient temperature (^{0}C)		
	20	30	40
0.02	25.68	25.08	24.49
0.03	24.33	23.82	23.35
0.04	23.32	22.79	22.31
0.05	22.61	22.05	21.55
0.06	22.10	21.52	20.99
0.07	21.71	21.11	20.56
0.08	21.41	20.79	20.23
0.09	21.17	20.54	19.97
0.10	20.97	20.33	19.75
0.11	20.80	20.16	19.57
0.12	20.67	20.01	19.41
0.13	20.55	19.88	19.28
0.14	20.44	19.77	19.17
0.15	20.35	19.68	19.07
0.16	20.27	19.59	18.98
0.17	20.20	19.51	18.90
0.18	20.14	19.45	18.83
0.19	20.08	19.39	18.77
0.20	20.03	19.34	18.71

Table B5: Effect of collector width on efficiency

Collector Width (m)	Efficiency, η, at different inlet temperature (^{0}C)		
	20	30	40
0.1	0.94	0.94	01.18
0.2	05.98	05.84	05.86
0.3	10.66	10.30	10.14
0.4	14.60	14.08	13.78
0.5	17.80	17.16	16.76
0.6	20.34	19.62	19.14
0.7	22.34	21.54	21.00
0.8	23.86	23.02	22.44
0.9	25.00	24.14	23.52
1.0	25.84	24.96	24.34
1.1	26.44	25.56	24.90
1.2	26.84	25.96	25.30
1.3	27.10	26.22	25.56
1.4	27.22	26.36	25.70
1.5	27.28	26.40	25.76
1.6	27.28	26.40	25.76
1.7	27.20	26.34	25.68
1.8	27.08	26.24	25.58
1.9	26.94	26.10	25.46
2.0	26.78	25.94	25.30

Table B6: Effect of collector length on efficiency

Collector Length (m)	Efficiency, η, at different inlet temperature (^{0}C)		
	20	**30**	**40**
0.2	08.81	08.57	08.32
0.3	15.30	14.95	14.61
0.4	21.00	20.53	20.07
0.5	25.70	25.11	24.55
0.6	29.54	28.87	28.21
0.7	32.66	31.90	31.16
0.8	35.17	34.34	33.54
0.9	37.16	36.28	35.43
1.0	38.74	37.82	36.92
1.1	39.96	39.01	38.08
1.2	40.91	39.93	38.98
1.3	41.61	40.62	39.65
1.4	42.12	41.12	40.13
1.5	42.49	41.48	40.48
1.6	42.72	41.71	40.71
1.7	42.79	41.78	40.79
1.8	42.81	41.80	40.81
1.9	42.84	41.80	40.82
2.0	42.84	41.81	40.82
2.1	42.79	41.79	40.82
2.2	42.75	41.77	40.81
2.3	42.69	41.76	40.79
2.4	42.48	41.65	40.66
2.5	42.48	41.49	40.51

Table B7: Effect of reduced temperature of efficiency

$\frac{(T_{in} - T_a)}{I}$	Efficiency, η, at different channel depths (m)		
	0.05	**0.10**	**0.15**
0.000	32.7000	31.5500	30.8700
0.002	31.6200	30.5400	29.9000
0.007	28.9800	28.0400	27.4800
0.012	26.3400	25.5400	25.0800
0.017	23.6600	23.0400	22.6600
0.022	21.0000	20.5200	20.2400
0.027	18.3400	18.0000	17.8200
0.032	15.6600	15.4800	15.3800
0.037	13.0123	12.9760	12.9731
0.042	10.3518	10.4660	10.5546
0.047	07.6913	07.9560	08.1361
0.052	05.0308	05.4460	05.7176
0.062	-0.2902	0.4260	0.8806
0.067	-2.9507	-2.0840	-1.5379

Appendix C: Constants used in the research

QUANTITY	CONSTANT VALUE
Wind velocity	1.5 m/s
Stefan–Boltzmann constant	5.57×10^{-8} $W/m^2 K^4$
thermal conductivity of the insulation	0.025 W/mK,
Absorber plate thermal emissivity	0.9
Glass thermal emissivity	0.85
Insulation thickness	0.05 m,
Absorptivity of the glass	0.06
The transmittance of the glass cover	0.9
Absorptivity of the absorber plate	0.9
Collector width	0.50 m
Collector tilt angle	15^0
Channel depth	0.15 m
Collector length	1 m

Appendix D: Publications and conference presentations

H. O. Ondieki, R. K. Koech, J. K. Tonui, S. K. Rotich. Theoretical analysis of a solar air heater with a rectangular air-flow duct under natural flow mode. *International Journal of thermal technologies. (accepted for publication)*

H. O. Ondieki, R. K. Koech, J. K. Tonui, S. K. Rotich. Mathematical modeling of a solar air collector with a trapezoidal corrugated absorber plate. *International Journal of Scientific and Technology Research. Vol. 3 No. 8, (2014)*

H. O. Ondieki, J. K. Tonui. A parametric study of a natural flow solar air heater with a rectangular air-duct profile. *African journal of Science, Technology, Innovations and Development.* vol 5 No.2 (97-102), 2013.

R. K. Koech, **H. O. Ondieki**, J. K. Tonui, S. K. Rotich. A steady state thermal model for photovoltaic/thermal (PV/T) system under various conditions. *International Journal of Scientific and Technology Research*. Vol. 1 (1-5), 2012.

R. K. Koech, **H. O. Ondieki,** J. K. Tonui, S. K. Rotich. Performance analysis of a PV/T air system based on heat transfer perspective. *International Journal of Scientific and Engineering Research.* Vol. 3, issue 10 (1-7), 2012.